Citation: Molecular Therapy—Nucleic Acids (2013) 2, e117; doi:10.1038/mtna.2013.46

www.nature.com/mtna

Improved Performance of Anti-miRNA Oligonucleotides Using a Novel Non-Nucleotide Modifier

Kim A Lennox[1], Richard Owczarzy[1], Derek M Thomas[1], Joseph A Walder[1] and Mark A Behlke[1]

Anti-microRNA oligonucleotides (AMOs) are steric blocking antisense reagents that inhibit microRNA (miRNA) function by hybridizing and repressing the activity of a mature miRNA. First generation AMOs employed 2′-*O*-Methyl RNA nucleotides (2′OMe) with phosphorothioate (PS) internucleotide linkages positioned at both ends to block exonuclease attack. Second generation AMOs improved potency through the use of chemical modifications that increase binding affinity to the target, such as locked nucleic acid (LNA) residues. However, this strategy can reduce specificity as high binding affinity compounds can bind to and suppress function of related sequences even if one or more mismatches are present. Further, unnatural modified nucleic acid residues can have toxic side effects. In the present study, a variety of non-nucleotide modifiers were screened for utility in steric blocking antisense applications. A novel compound, N,N-diethyl-4-(4-nitronaphthalen-1-ylazo)-phenylamine ("ZEN"), was discovered that increased binding affinity and blocked exonuclease degradation when placed at or near each end of a single-stranded oligonucleotide. This new modification was combined with the 2′OMe RNA backbone to make ZEN-AMOs. The new ZEN-AMOs have high potency and can effectively inhibit miRNA function *in vitro* at low nanomolar concentrations, show high specificity, and have low toxicity in cell culture.

Molecular Therapy—Nucleic Acids (2013) **2**, e117; doi:10.1038/mtna.2013.46; published online 27 August 2013
Subject Category: Antisense oligonucleotides siRNAs, shRNAs, and miRNAs

Introduction

MicroRNAs (miRNAs) are important small noncoding RNAs responsible for spatiotemporally fine tuning gene expression at the post-transcriptional level. Typically 20–24 nucleotides long, these small RNA molecules regulate gene expression through imperfect base pairing in the 3′UTR of targeted genes, leading to mRNA degradation or preventing protein synthesis.[1] Just about every cellular biological process, including cell differentiation, apoptosis, and proliferation, is controlled by the miRNA regulatory network.[2,3] The wide acknowledgement of miRNAs as effective biological regulators has amplified the need for techniques to overexpress or inhibit their function both to investigate function as well as for therapeutic purposes to correct diseases associated with miRNA dysregulation.[4]

The standard method used today to inhibit miRNA function is the administration of a synthetic anti-miRNA oligonucleotide (AMO) which has perfect complementarity to the full-length mature miRNA target. AMOs are a version of steric blocking antisense oligonucleotides that form a duplex with the miRNA guide strand and this binding event is the basis for miRNA inactivation. Inactivation requires that binding affinity between the miRNA and the AMO is significantly higher than that of the natural miRNA guide strand/passenger strand interaction; inhibition of miRNA activity requires that the AMO can hybridize to the miRNA guide strand whether it exists in single-stranded form, double-stranded form with the natural passenger strand (which will require invasion of a pre-existing duplex), or bound to an Argonaute protein in the miRNA induced silencing complex (miRISC). It has long been appreciated that chemical modifications which increase duplex stability usually increase the potency of antisense oligonucleotides, whether used in steric blocking[5–7] or RNase H degradative modes of action.[8,9] The binding affinity of an AMO must be sufficiently high that it cannot be removed from the miRNA target by helicase activities present in miRISC or by competition from other natural targets within the cell. In addition to having high binding affinity, the AMO must be nuclease resistant so that it is not degraded by extra- or intracellular nucleases, including the endonuclease activity of Argonaute 2 (Ago2) in miRISC. Several AMO designs which satisfy most of these criteria have been developed and have been used with good results to inhibit miRNA function both *in vitro* and *in vivo*.[4,6,7]

An ideal AMO would have: (i) high affinity to the target to improve potency, (ii) resistance to both exo- and endonuclease attack, (iii) low toxicity, (iv) high specificity, and (v) a relatively low cost for synthesis. High affinity to the target miRNA can be achieved through use of base modifications, sugar modifications, or addition of certain non-nucleotide modifiers. It would be advantageous if the same modification that increased binding affinity also contributed to improved nuclease resistance. Modifications to the heterocyclic bases can increase binding affinity but do not increase nuclease resistance. Substitution of 5-methyl-2′-deoxycytidine (5-Me-dC) for 2′-deoxycytidine (dC) can increase T_m by 0.5 °C, however this small change is usually insufficient to make a significant impact on potency. The propynyl pyrimidines (5-propynyl-dU and 5-propynyl-dC) can increase T_m by 1.7–2.5 °C per insertion and were originally hoped to be useful reagents for antisense applications.[10] However, these modifications

[1]Integrated DNA Technologies, Inc., 1710 Commercial Park, Coralville, Iowa City, USA. Correspondence: Mark A Behlke, Integrated DNA Technologies, 1710 Commercial Park, Coralville, IA 52241, USA. E-mail: mbehlke@idtdna.com
Keywords: AMO; antagomir; anti-miRNA; antisense; miRNA; oligonucleotide; RNAi; ZEN
Received 14 February 2013; accepted 24 June 2013; advance online publication 27 August 2013 doi:10.1038/mtna.2013.46

have severe toxicity when used *in vivo*.[11] Another base modification, AP-dC ("G-clamp") can increase T_m by 7.5 °C per insertion but its use was found to actually reduce activity of antisense oligonucleotides *in vivo*.[12]

2′-modification of the ribose can increase both T_m and improve nuclease resistance. 2′-*O*-Methyl RNA (2′OMe) is a nontoxic naturally occurring nucleic acid which confers resistance to degradation by mammalian endonucleases and provides a large increase in binding affinity to an RNA target compared with DNA. However, 2′OMe oligonucleotides remain sensitive to exonuclease degradation and must be protected at their ends with additional chemical modification(s), such as phosphorothioate (PS) linkages, to perform well in cell culture or *in vivo*.[6] Alternatively, addition of long terminal hairpin structures can block exonuclease attack without the need for other chemical modifications.[13,14] The first AMOs effectively used *in vivo* were called "antagomirs". This design employed 2′OMe residues modified with several PS linkages at both ends and a 3′-cholesterol modifier to facilitate uptake. The combination of 2′OMe residues with a limited number of PS linkages minimized toxicity and resulted in an AMO that was protected from both exo- and endonuclease degradation and had high specificity.[6,15,16] Unfortunately, the antagomir design had relatively low potency and required very high dosing (up to 80 mg/kg *in vivo*).

AMOs containing 2′-Fluoro (2′F) nucleotides can have higher potency than the original 2′OMe antagomirs (*in vivo* dosing around 5–12.5 mg/kg), benefitting from the T_m-enhancing properties of this modification.[17–19] Unfortunately, the 2′F modification offers little improvement in nuclease resistance in single-stranded form and requires full PS modification throughout the phosphate backbone; the most effective designs also incorporate the addition of other 2′-modified residues at the ends, such as locked nucleic acid (LNA) or 2′-methoxyethyl (2′MOE) nucleotides. This modification is also relatively expensive, which further limits its utility. LNA residues show the highest T_m-enhancement of any commonly used modification and also confer some degree of nuclease resistance, but still benefit from PS modification. The LNA modification has been used to make very potent AMOs (*in vivo* dosing around 5–25 mg/kg in rodents or as low as 2 mg/kg in nonhuman primates).[20–22] For routine research use, LNAs are often placed in the context of a DNA or a 2′OMe backbone at every third position.[6,23] Limiting LNA content reduces the likelihood of undesired hairpin and self-dimer hybridization that often comes with incorporating high binding affinity modifications into oligonucleotides. While overall a very useful modification, adverse outcomes can occur from use of LNAs in AMOs due to off-target effects caused by unintended binding to a nontargeted miRNA or due to direct chemical toxicity of LNA nucleotides. As few as four LNA nucleotides in an 18mer oligonucleotide can cause severe hepatotoxicity *in vivo*;[24] this toxicity varies with sequence context and its mechanism is unknown so empiric testing is needed to determine if a given sequence is toxic.[12] Nevertheless, some LNA-modified AMOs can be safely administered *in vivo*, usually using designs that have been carefully optimized and are shorter than the full length miRNA.[20–22] For example, a 15mer miR-122 DNA/LNA-PS AMO (SPC3469) was recently demonstrated to have a favorable toxicity profile in nonhuman primates and this compound is under development for use as a human therapeutic.[25]

A variety of approaches can be taken to block nuclease degradation of a synthetic oligonucleotide including modification of the internucleotide linkages, alterations to the structure of the sugar backbone, or addition of non-nucleotide modifiers at or near the oligonucleotide termini. The PS modification substitutes sulfur for a nonbridging oxygen in the phosphate backbone and has long been used to protect synthetic oligonucleotides from nuclease degradation. The PS modification also makes the oligonucleotides more hydrophobic, leading to nonspecific protein binding.[26,27] While this can lead to some undesired off-target effects,[28] it also improves pharmacodynamics by enhancing binding to serum proteins and reducing the otherwise rapid renal excretion of oligonucleotides when administered *in vivo*.[29] Unfortunately, PS linkages also decrease the T_m of the oligonucleotide,[30] which reduces potency of AMOs. The PS modification is therefore most effective when used in combination with other modifications that increase binding affinity. Another drawback of the PS linkage is that it introduces a new chiral center into the molecule. An oligonucleotide containing "N" PS linkages is actually a mixture of 2^N distinct diasteriomers, each potentially having different biological activity and toxicity. Other alterations to the internucleotide linkages can confer nuclease resistance, such as the methylphosphonate or phosphoramidate modifications. Like the PS modification, these also significantly lower oligonucleotide binding affinity and introduce a new chiral center.[31]

Modification of the 2′-position of the ribose sugar backbone can confer improved nuclease stability, as discussed above for 2′OMe RNA, 2′F RNA, and LNA residues. We chose to focus on use of 2′OMe RNA as the starting point for a new generation of AMOs for several reasons: 2′OMe RNA has no significant toxicity, has a relatively high binding affinity for RNA, and costs approximately the same to manufacture as RNA. The primary drawback for use of 2′OMe RNA as an AMO is that, although it is naturally resistant to mammalian endonucleases, it is susceptible to attack by serum and cellular exonucleases.[6] Therefore additional modifications must be employed at or near the 5′- and 3′-termini to block exonuclease attack. It would be beneficial if such modifications also increased binding affinity of the AMO to the miRNA target, did not produce a mixture of diasteriomers and was nontoxic to mammalian cells. A novel compound, N,N-diethyl-4-(4-nitronaphthalen-1-ylazo)-phenylamine ("ZEN"), was identified that met all of these criteria. New ZEN-AMOs were synthesized placing the modifier at or near both ends of a phosphodiester 2′OMe oligonucleotide complementary to a targeted miRNA. The new design showed significantly higher potency than the original 2′OMe-PSends antagomir design. Potency was equal to DNA/LNA PS chimeras yet showed none of the toxicity commonly associated with these compounds. This new design should prove useful as an *in vitro* tool to suppress miRNA activity. Testing is ongoing to determine potential utility *in vivo*.

Results

The ZEN modifier

A series of chemical modifying groups were screened for the ability to increase T_m when placed internally within a nucleic acid sequence.[32] All modifiers were incorporated as phosphoramidites using normal phosphodiester linkages between

nucleotides. Modifications were incorporated as either a substitution where the modifier replaced a nucleoside in one strand of the duplex or as an insertion where the modifier was placed between adjacent residues. In addition to the control unmodified duplex, a C3 spacer modifier (propanediol) was used to establish a baseline for the thermodynamic effects of the other modifications studied; this modification represents addition of a phosphate group and three carbon backbone, spatially mimicking addition of a ribose. Modifiers were placed at various positions in a short 10mer DNA oligonucleotide, hybridized to an unmodified 10mer DNA complement, and T_m was measured in a 1 mol/l NaCl environment. All of the modifiers reduced T_m when placed as a substitution for a nucleotide. While most of the modifiers also lowered the T_m of the DNA duplexes when placed as an insertion, N,N-diethyl-4-(4-nitronaphthalen-1-ylazo)-phenylamine ("ZEN") was found to have a unique stabilizing effect on hybridization. This structure, which has the additional properties of being a "dark quencher", was first identified as a potential compound of interest in previous screens performed to find new modifications that improved performance of dual-labeled fluorescence-quenched probes.[32] The structure of the ZEN modification is shown in **Figure 1**. The relative T_m effect of insertion or substitution of a ZEN modifier compared with a C3 spacer is shown in **Supplemental Table S1**, online. Depending on position in the 10mer duplex, as an insertion the ZEN modifier increased T_m by +2.4 to +7.9 °C whereas effects of the C3 spacer modifier varied from –11.3 to +0.7 °C. The greatest T_m increase was seen when a ZEN group was positioned at the penultimate position between the last and next to last nucleotide on both ends of the oligonucleotide (+11.0 °C). Preliminary experiments performed on the short DNA 10mers indicated that the ZEN modifier blocked exonuclease attack (data not shown). We next studied the properties of the ZEN modifier when used in the context of a 2′OMe 22mer miR-21 AMO.

Nuclease stability of ZEN-modified 2′OMe AMOs

To have high potency and sustained activity, AMOs must survive transient exposure to serum (during delivery) and long-term exposure to cytoplasm. The primary nuclease activity present in serum is a 3′-exonuclease[33] whereas cytoplasm contains endonucleases, 5′-exonucleases, and 3′-exonucleases. 2′OMe oligonucleotides inherently show resistance to cellular endonucleases but are susceptible to exonuclease attack.[6] Fortuitously, the ZEN modifier confers a significant increase in T_m when placed between terminal residues (**Supplemental Table S1**, online) where it is also most likely to be useful as a modifier to block exonuclease attack. As a unified nomenclature, we will henceforth call modification with ZEN between the last and next to last nucleotide at the 3′-end "3′inZEN" (3′-internal-ZEN) and with ZEN as a terminal modifier after the final 3′-nucleotide "3′ZEN". Similar nomenclature is employed for the C3 spacer modifier ("3′inC3" vs. "3′C3") and for modification of the 5′-end. A series of miR-21 AMOs were synthesized using DNA or 2′OMe RNA, with or without the addition of PS linkages, ZEN, or C3 spacer modifiers. Nuclease stability of the various AMO designs was studied by incubation in 10% fetal bovine serum (FBS) or in 20% liver cell protein extract. Following incubation, AMO integrity was evaluated by denaturing polyacrylamide gel electrophoresis and the results are shown in **Figure 2a** (FBS) and **Figure 2b** (liver protein extract); sequences are shown in **Figure 3**. The resulting degradation products were identified using electrospray-ionization mass spectrometry (ESI-MS), shown in **Supplemental Table S2**, online (FBS) and **Supplemental Table S3**, online (liver protein extract). The same set of experiments were also performed using 50% FBS and 50% liver cell protein extract with identical results (data not shown).

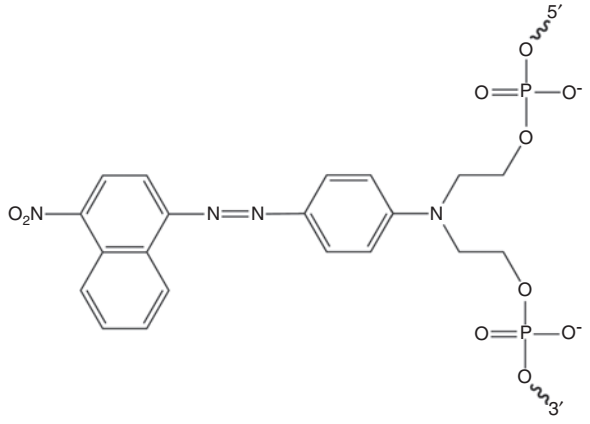

Figure 1 Structure of the ZEN modifier. N,N-diethyl-4-(4-nitronaphthalen-1-ylazo)-phenylamine is connected via phosphate linkages to the ribose backbone of the oligonucleotide.

The unmodified DNA AMO ("DNA") was rapidly degraded in both serum and liver cell extract. When protected from exonuclease attack by addition of the ZEN modifier on both ends ("DNA 5′inZEN, 3′ZEN"), the DNA AMO was still rapidly degraded in cell extract but remained mostly intact following incubation in serum for up to 24 hours. This finding is consistent with prior reports that serum contains a 3′-exonuclease activity while cell extracts contain multiple nuclease activities, including endonucleases.[6,33] The unmodified 2′OMe AMO ("2′OMe") was also degraded in both serum and cell extract, but degradation proceeded less rapidly than for the DNA AMO. On ESI-MS, all of the identifiable surviving fragments were 3′-truncations, consistent with attack by a 3′-exonuclease (serum > cell extract). Protection of only the 5′-end with an internal ZEN modifier ("2′OMe 5′inZEN") did not improve stability in either serum or cell extract; however, 5′-modification is still useful as it can contribute to long-term stability by inhibiting low levels of 5′-exonuclease activity present in cytoplasm (see below). Protection of the 3′-end of a 2′OMe AMO is therefore critical to survive exposure to both serum and the intracellular environment.

Placing a non-nucleotide modifier such as ZEN or a C3 spacer (propanediol) between the next to last and 3′-terminal nucleotide of a 2′OMe AMO blocked processive 3′-exonuclease action but left the 3′-terminal nucleotide susceptible to attack ("2′OMe 5′inC3, 3′inC3" and "2′OMe 5′inZEN, 3′inZEN"). Both oligonucleotides having this design were reduced from 22mer to 21mer size in serum and cell extract, showing loss of their 3′-terminal nucleotide on ESI-MS. It is interesting that the exonuclease activity was able to attack the phosphate linkage at the 5′-side of a 2′OMe residue, adjacent to the non-nucleotide modifier,

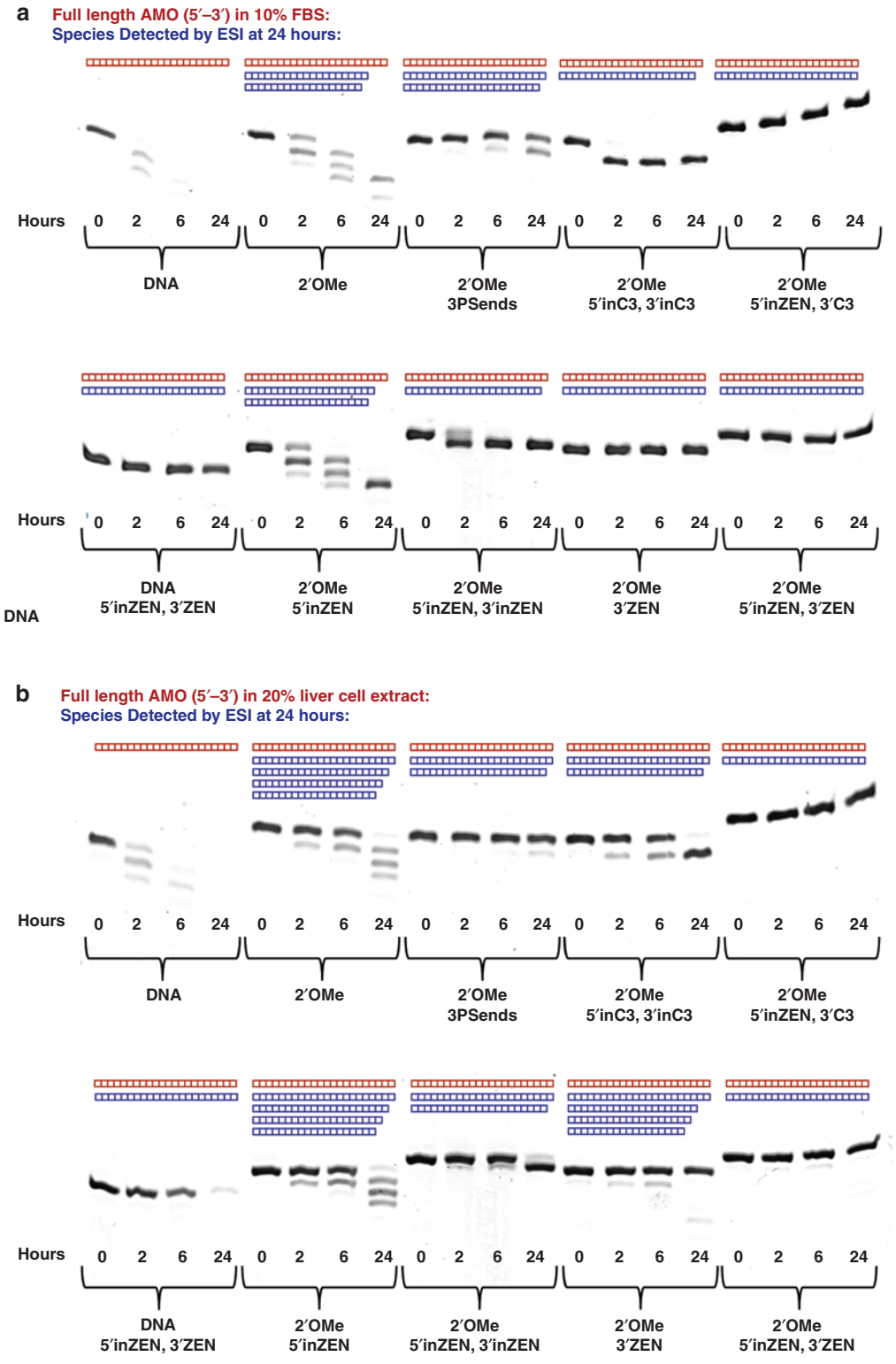

Figure 2 Degradation studies of chemically modified oligonucleotides. 2′OMe AMOs were studied to assess the effects that various end-modifications have on nuclease stability. Two DNA AMOs were included as positive controls for nuclease activity. 1.1 nmoles of each AMO (sequences shown are in **Figure 3**) was incubated in (**a**) 10% FBS or (**b**) 20% mouse liver protein extract at 37 °C for 0, 2, 6, or 24 hours. Each AMO was separated on denaturing polyacrylamide gels and stained with methylene blue. The 24-hour digests were analyzed using ESI-LC-MS and species detected are reported above their respective gel images. Each "box" represents one nucleotide; red boxes indicate the full-length 22-mer AMO and blue boxes represent all degradation products identified, which were truncations from the AMO 3′ ends. See **Supplemental Tables S2, S3**, online for more detailed degradation results. AMO, Anti-microRNA oligonucleotides.

Name	miR-21 AMO Sequences (5′–3′)[a]	T_m (°C)[b]	ΔT_m (°C)[c]	$\Delta G°_{37}$ (kcal/mol)	K_a(37 °C)[d] (mol/l)$^{-1}$
DNA	t c a a c a t c a g t c t g a t a a g c t a	56.3	–16.4	–18.7	1.5×10^{13}
DNA 5′inZEN, 3′ZEN	tzc a a c a t c a g t c t g a t a a g c t az	60.3	–12.4	–19.1	3.0×10^{13}
2′OMe	U C A A C A U C A G U C U G A U A A G C U A	72.7	–	–26.9	9.4×10^{18}
2′OMe 3PSends	U*C*A*A C A U C A G U C U G A U A A G*C*U*A	72.2	–0.5	–26.4	4.3×10^{18}
2′OMe PS	U*C*A*A*C*A*U*C*A*G*U*C*U*G*A*U*A*A*G*C*U*A	68.1	–4.6	ND[e]	ND
2′OMe 3′inZEN	U C A A C A U C A G U C U G A U A A G C UzA	73.4	0.7	–26.7	6.3×10^{18}
2′OMe 3′ZEN	U C A A C A U C A G U C U G A U A A G C U Az	74.0	1.3	–27.9	4.8×10^{19}
2′OMe 5′inZEN	UzC A A C A U C A G U C U G A U A A G C U A	75.4	2.7	–28.9	2.3×10^{20}
2′OMe 5′inZEN, 3′C3	UzC A A C A U C A G U C U G A U A A G C U A^	ND	ND	ND	ND
2′OMe 5′inZEN, 3′inZEN	UzC A A C A U C A G U C U G A U A A G C UzA	76.2	3.5	–30.1	1.6×10^{21}
2′OMe 5′inZEN, 3′ZEN	UzC A A C A U C A G U C U G A U A A G C U Az	76.3	3.6	–30.6	3.8×10^{21}
2′OMePS 5′inZEN, 3′inZEN	UzC*A*A*C*A*U*C*A*G*U*C*U*G*A*U*A*A*G*C*UzA	71.4	–1.3	ND	ND
2′OMe 3′inC3	U C A A C A U C A G U C U G A U A A G C U^A	72.0	–0.7	–26.3	3.2×10^{18}
2′OMe 5′inC3	U^C A A C A U C A G U C U G A U A A G C U A	72.0	–0.7	–26.5	4.8×10^{18}
2′OMe 5′inC3, 3′inC3	U^C A A C A U C A G U C U G A U A A G C U^A	71.7	–1.0	–26.9	9.2×10^{18}
2′OMe 5′inC3, 3′C3	U^C A A C A U C A G U C U G A U A A G C U A^	72.3	–0.4	–26.8	7.7×10^{18}
DNA/LNA PS	t*C*a*a*C*a*t*C*a*g*T*c*t*G*a*t*A*a*g*C*t*a	74.5	1.8	ND	ND
2′OMe/LNA PS	U*C*A*A*C*A*U*C*A*G*T*C*U*G*A*U*A*A*G*C*U*A	87.3	14.6	ND	ND

[a]Lowercase red = DNA; Uppercase black = 2′OMe; Uppercase black underscore = LNA; "*" = PS linkage; "z" = ZEN; "^" = C3 spacer

[b]Oligonucleotides were annealed to complementary RNA strand, 5′ -pUAGCUUAUCAGACUGAUGUUGA-3′ (p = phosphate), in 150 mmol/l Na^+ buffer.

[c]ΔT_m = [T_m (Test AMO)] - [T_m(2′OMe AMO)].

[d]Equilibrium constant for association of the oligonucleotide with the complementary RNA strand.

[e]ND = Not determinded

Figure 3 Effect of modification on the T_m's and binding affinities of miR-21 AMOs. AMOs were annealed to a synthetic RNA oligonucleotide mimic of miR-21 and T_m's were measured in 150 mmol/l NaCl. $\Delta G°_{37}$ values and binding affinities were determined from analysis of the shape of the melt curves.[38] AMO, Anti-microRNA oligonucleotides.

but was not able to attack the phosphate linkage at the 5′-side of the modifier. Placing the non-nucleotide modifier as a 3′-terminal modification (at the end of the oligonucleotide, not between terminal nucleotides) provided complete protection of the 2′OMe AMO ("2′OMe 3′ZEN") in serum, although some degradation was still observed in cell extract. The greatest stability was achieved using a combination of both 5′- and 3′-modifications, where the 3′-modification was placed at the very 3′-terminus of the oligonucleotide. The two AMOs of this design studied ("2′OMe 5′inZEN, 3′C3" and "2′OMe 5′inZEN, 3′ZEN") were totally resistant to degradation in both serum and cell extract.

The original antagomir AMO design employed several PS linkages at both ends of a 2′OMe oligonucleotide to provide protection from exonucleases.[15,16] In the present study, a 2′OMe miR-21 AMO with three PS bonds on each end ("2′OMe 3PSends") was found to have increased stability in both serum and cell extract; however, some fraction of the material showed loss of a single nucleotide at the 3′-end consistent with 3′-exonuclease attack (serum > cell extract). This likely occurs due to the presence of mixed *Rp* and *Sp* stereoisomers of the PS bond, which show differential resistance to nuclease attack. Replacement of a single sulfur atom for one of the nonbridging oxygen atoms in the phosphate bond creates a chiral center at the modified phosphate and the resulting two stereoisomers, *Rp* and *Sp*, often show differential effects when the nucleic acid substrate is subjected to attack by various nucleases. For example, when a PS linkage is placed immediately 3′- to an RNA residue (the common cleavage site for single-strand specific ribonucleases), the *Sp* isomer confers significantly greater resistance to cleavage by RNase A and snake venom phosphodiesterase than does the *Rp* isomer.[34,35] In contrast, spleen phosphodiesterase cleaves the *Sp* PS isomer preferentially.[36] In addition to failing to completely block 3′-exonuclease degradation, the PS-end block approach also lowers the T_m of the antagomir, leading to reduced potency (see below).

Sustained function of an AMO requires that the oligonucleotide remain intact in cytoplasm for many days. Stability of various AMO designs (**Supplemental Figure S1A**, online) were studied following 96 hour incubation in liver cell extracts. As before, degradation products were analyzed by polyacrylamide gel electrophoresis (**Supplemental Figure S1B**, online) and ESI-MS (data not shown). As expected, the positive control samples for endonuclease activity ("DNA 5′inZEN, 3′ZEN") and exonuclease activity ("2′OMe") were almost completely degraded by 96 hours. The miR-21 "2′OMe 5′inZEN, 3′inZEN" AMO showed loss of the 3′-residue but was otherwise intact. The miR-21 "2′OMe 3′ZEN" AMO showed around a 50% mass loss but the remaining material was mostly full length; a small amount of (*n*–1)mer material was seen by ESI-MS indicating weak 5′-exonuclease activity (data not shown). Only the miR-21 "2′OMe 5′inZEN, 3′ZEN" AMO was completely intact after the 4 days of incubation. To confirm that the "2′OMe 5′inZEN, 3′ZEN" modification pattern was protective in different sequence contexts, AMOs of this

design were made specific for miR-17-5p, miR-24, miR-31, miR-125b, miR-155, and miR-331. All survived incubation for 4 days in liver protein extract with no evidence of degradation.

Effects of the ZEN modification on AMO T_m and binding affinity

The ZEN modification was initially identified by its ability to increase T_m when incorporated into a short DNA duplex. Relative effects on T_m may be different in the context of a 2′OMe oligonucleotide hybridized to an RNA target. Further, the increase in T_m that results from addition of one to two modifying groups for 22mer duplexes, which start with a much higher T_m, is expected to be lower than what was seen previously for a 10mer DNA duplex (**Supplementary Table S1**, online). Melting studies were performed to determine the effects that ZEN and other modifications have on the T_m of a series of miR-21 AMOs. The AMOs were 22mers comprising DNA, 2′OMe, or LNA residues combined with ZEN, C3 spacer, or PS modifications; this set of oligonucleotides was duplexed with a miR-21 mimic (22mer RNA oligonucleotide with 5′-phosphate). Melting studies were performed in a buffer containing 150 mmol/l Na^+ cation, which is relatively similar to intracellular monovalent cation conditions. Results are shown in **Figure 3**.

The unmodified "2′OMe" miR-21 AMO had a T_m of 72.7 °C while the same sequence as "DNA" had a T_m of 56.3 °C, a differential of 16.4 °C. As expected, the PS modification reduced T_m: the AMO with six PS linkages ("2′OMe 3PSends") had a T_m of 72.2 °C (ΔT_m = –0.5 °C) and the fully modified AMO with 21 PS linkages ("2′OMe PS") had a T_m of 68.1 °C (ΔT_m = –4.6 °C). Addition of a ZEN group at the 3′-end either as an internal insertion between the terminal nucleotides ("2′OMe 3′inZEN") or as a terminal modifier ("2′OMe 3′ZEN") increased T_m by similar amounts (ΔT_m = +0.7 or +1.3 °C). Interestingly, addition of a ZEN group at the 5′-end ("2′OMe 5′inZEN") had a larger effect (ΔT_m = +2.7 °C). From T_m measurements done in other sequence contexts, it appears this is a general phenomenon and that ZEN usually increases duplex stability more when placed at the 5′-end than at the 3′-end of an AMO (data not shown). Dual modification with ZEN at both the 5′- and 3′-ends showed additive effects ("2′OMe 5′inZEN, 3′inZEN" and "2′OMe 5′inZEN, 3′ZEN") with measured T_m values of 76.2 and 76.3 °C, respectively (ΔT_m = +3.5 or +3.6 °C). Compared with the antagomir design ("2′OMe 3PSends"), which had lower T_m due to the 6 PS modifications, the dual-ZEN AMO showed a T_m increase of 4 °C. Interestingly, dual-ZEN modification of the DNA AMO ("DNA 5′inZEN, 3′ZEN") showed a 4 °C increase in T_m compared with the unmodified DNA AMO. Thus, similar effects were seen between incorporation of the ZEN modification in a DNA oligonucleotide and in a 2′OMe oligonucleotide. The C3 spacer modifier was incorporated into the 2′OMe AMO using the same modification patterns and studied in a similar fashion. In all cases, a slight decrease in T_m was observed. Thus, while this non-nucleotide modifier can be used like ZEN to block exonuclease attack, it does not improve duplex stability.

A DNA/LNA chimera was studied having an alternating pattern of two DNAs followed by one LNA residue (incorporating a total of seven LNAs). Due to the susceptibility of DNAs to endonuclease attack, this AMO was made using full PS modification.[6] The "DNA/LNA PS" AMO showed a T_m of 74.5 °C, slightly lower than the dual-ZEN AMOs, but still 2.3 °C higher than the "2′OMe 3PSends" design and fully 18.2 °C higher than the unmodified DNA AMO. A 2′OMe/LNA chimera with the same alternating modification pattern was also studied ("2′OMe/LNA PS"). This AMO showed the highest T_m of the series, 87.3 °C, which is 11 °C higher than the dual-ZEN AMO and 14.6 °C higher than the unmodified "2′OMe" AMO, demonstrating the large increases in duplex stability that can be achieved using the LNA modification in combination with 2′OMe residues.

The ability of an AMO to suppress miRNA function relates to the relative duplex stability and binding affinity of the oligonucleotide to the complementary RNA strand under physiological conditions. The best measure of relative affinity is the free energy of the annealing reaction at 37 °C rather than the T_m value.[37] We therefore estimated the standard free energy change and the corresponding equilibrium constant for the annealing reaction at 37 °C from the shapes of the melting curves for each duplex as described by Marky.[38] Results are shown in **Figure 3**. Due to the large number of different species present in the fully PS-modified AMOs (a random mix of *R* and *S* isomers should be present at each chiral thiophosphate group, resulting in a total of 2^{21} possible variants in a 22mer oligonucleotide), these AMOs showed wider melt curves and accurate free energies could not be determined from melt curve fits. Although the T_m changes caused by different modifications appear small, they nevertheless correspond to large differences in the relative binding affinities at 37 °C.[37,39] For example, comparison of the "2′OMe 5′inZEN, 3′ZEN" AMO (T_m = 76.3 °C) with the "2′OMe 3PSends" AMO (T_m = 72.2 °C) shows a ΔT_m of only 4.1 °C yet the binding constant (K_a) of the dual-ZEN AMO at 37 °C is about 900-times larger than that of the "2′OMe 3PSends" AMO. Indeed, to function as a miRNA inhibitor the AMO must bind to and inactivate the target miRNA in competition with the miRNA binding to its native guide strand or target mRNAs in miRISC. The calculated 900-fold higher binding affinity of the "2′OMe 5′inZEN, 3′ZEN" AMO compared with the "2′OMe 3PSends" AMO indicates that the new design should function as a better miRNA inhibitor.

Potency of ZEN-AMOs

Functional potency of different AMO designs were studied using a previously validated luciferase reporter system.[6] Briefly, a perfect match binding site for hsa-miR-21 was cloned into the 3′UTR of *Renilla* luciferase (RLuc) in the PsiCHECK-2 vector which also expresses firefly luciferase (FLuc) for use as an internal normalizing transfection control. When this reporter plasmid is transfected into HeLa cells, *Renilla* luciferase expression is suppressed by endogenous miR-21. Blocking miR-21 using an AMO de-represses RLuc to a level that directly relates to the potency of the AMO. A large dynamic range and high sensitivity is achieved due to the high level of expression of miR-21 in this cell type. Except for the two DNA oligonucleotides, which show no anti-miR-21 activity, and the "2′OMe 5′inZEN, 3′C3" AMO, the set of AMOs shown in **Figure 3** was tested for potency at doses ranging from 0.3 to 30 nM. AMO transfections are typically

done either as a 6-hour transfection followed by washing the cells and media change (this protocol is preferred when the cell type employed shows toxicity with the transfection agent/AMO chemistry combination) or as a 24-hour transfection with no media change. In either case, miR-21 activity is measured 24 hours post-transfection. The relative potency of the various AMOs was similar using the two-transfection protocols. Overall, a higher level of miRNA inhibition is achieved using the 24-hour transfection; however, differences in potency between the AMO designs are more obvious using the 6-hour transfection. Therefore, results using both methods are shown, the 6-hour transfection in **Figure 4a** and the 24-hour transfection in **Figure 4b**.

The unmodified "2′OMe" AMO showed low activity, most likely due to exonuclease degradation; the fully PS-modified version ("2′OMe PS") also showed low activity, probably due to reduced binding affinity from the 21 PS linkages. The original antagomir design, 2′OMe with only three PS linkages on each end, showed improved activity, especially with the 24-hour transfection protocol. Interestingly, ZEN modification of the 3′-end ("2′OMe 3′inZEN" and "2′OMe 3′ZEN") resulted in only a modest increase in activity while ZEN modification

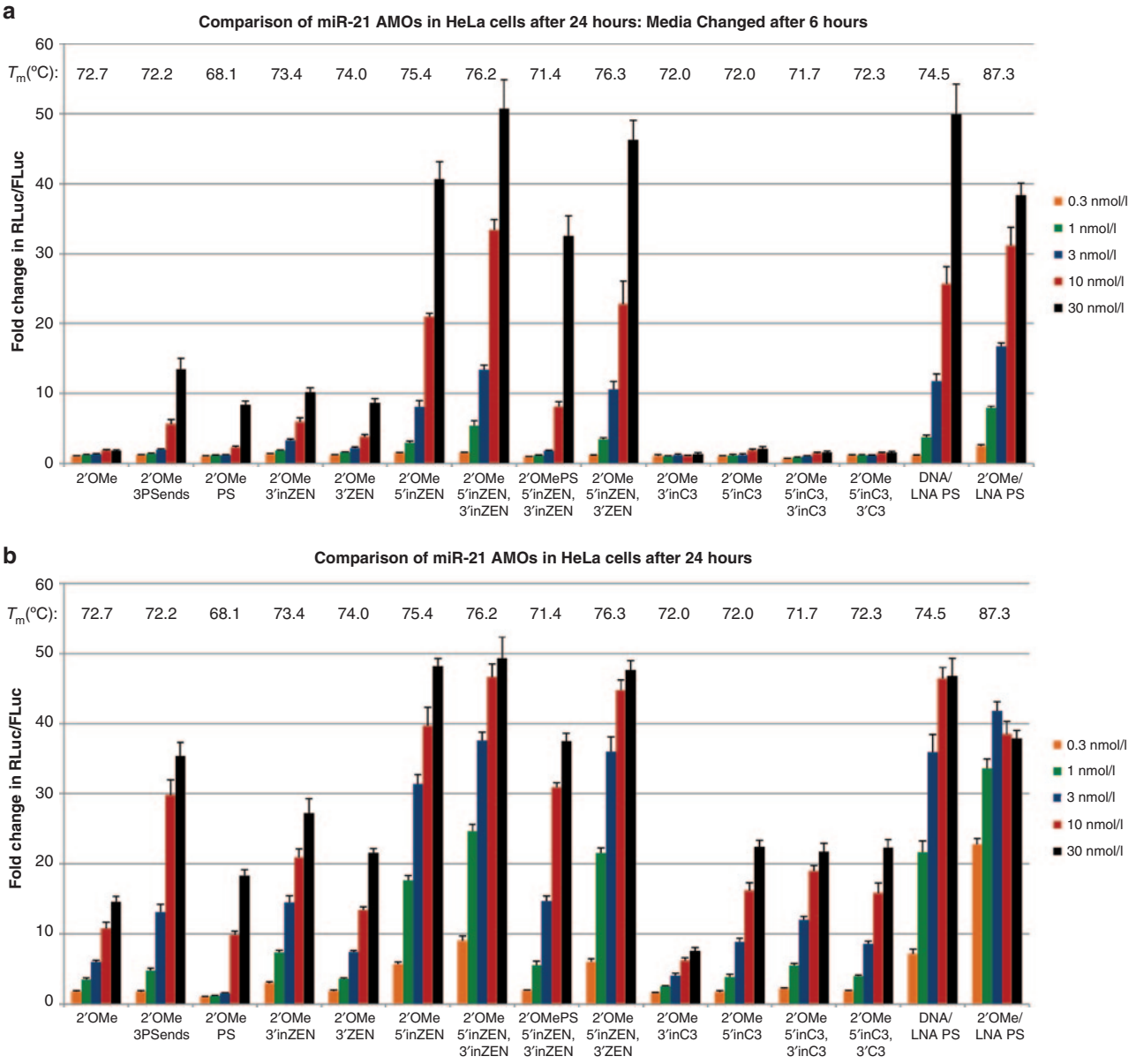

Figure 4 Potency profiles of miR-21 AMOs in HeLa cells. (**a**) AMOs targeting miR-21 were designed with various chemical compositions and transfected at concentrations ranging from 0.3 to 30 nmol/l into HeLa cells expressing the psiCHECK-miR-21 plasmid (**a**) with the media changed 6 hours post-transfection, or (**b**) with no change in media. Cells were lysed and analyzed for luciferase activity 24 hours post-transfection. All values were normalized with the internal firefly luciferase (FLuc) control and reported as a fold change in *Renilla* luciferase (RLuc) compared with the lipid reagent control, which was set at 1. T_m values from **Figure 3** are aligned above their respective potency profiles. AMO, Anti-microRNA oligonucleotides.

of the 5′-end ("2′OMe 5′inZEN") led to a large increase in activity. This may relate to the greater binding affinity seen with the 5′-ZEN modification compared with the 3′-ZEN modification (**Figure 3**), in spite of the benefits gained by blocking 3′-exonuclease attack through the 3′-ZEN modification. However, the same effect was observed for the C3 spacer modified AMOs: 5′-end modification increased potency more than 3′-end modification ("2′OMe 5′inC3" vs. "2′OMe 3′inC3", 24-hour transfection). In this case, the two AMO variants had the same T_m (72 °C) yet the 5′-modified variant showed higher potency, in spite of the expectation that the 3′-modified variant should be more stable in serum and cell extract. Therefore, there may some benefit to modification of the 5′-end of the AMO (which binds the 3′-end of the target miRNA), unrelated to nuclease resistance and binding affinity to the target miRNA; we speculate that this may relate to the ability of the AMO to invade miRISC.

Modification of both ends of the AMO with ZEN led to even greater increases in potency ("2′OMe 5′inZEN, 3′inZEN" and "2′OMe 5′inZEN, 3′ZEN"). Curiously, for the miR-21 target, the "2′OMe 5′inZEN, 3′inZEN" AMO showed slightly higher potency than the "2′OMe 5′inZEN, 3′ZEN" variant. Following transfection, AMOs modified with 3′-internal-ZEN were expected to lose the 3′-terminal nucleotide to exonuclease attack (**Figure 2a**, **b**) while the 3′-ZEN was expected to protect the 3′-end. It is therefore counterintuitive that the 3′-internal-ZEN variant should be more potent, yet this observation held true over three separate experiments, each of which included three biological replicates. The dual-modified AMOs containing C3 spacer modifiers did not show much improvement in potency ("2′OMe 5′inC3, 3′inC3" and "2′OMe 5′inC3, 3′C3") over the unmodified "2′OMe" AMO, demonstrating the benefit gained from the increased binding affinity imparted by the ZEN modification. Full PS modification of the dual-ZEN AMO ("2′OMePS 5′inZEN, 3′inZEN") decreased activity compared with the phosphodiester version, as expected due to the decrease in binding affinity that results from the PS modification. However, the "2′OMePS 5′inZEN, 3′inZEN" AMO showed much greater activity than the same oligonucleotide lacking the ZEN modification ("2′OMePS"). Addition of a third ZEN modification placed centrally in the ZEN-AMO decreased miR-21 inhibition, suggesting that there may be a limit on the number of ZEN modifiers placed this closely together (data not shown).

LNA/DNA chimeras are among the most commonly used AMO variants today. Potency of the dual-ZEN AMOs was nearly identical to the "DNA/LNA PS" AMO. The 2′OMe/LNA chimera is a less commonly used AMO design, but was shown to have very high potency in earlier studies.[6,23] Indeed, this design showed the highest potency of any of the miR-21 AMOs tested, which correlated with its very high T_m of 87 °C. This high potency, however, comes at the cost of decreased specificity (see below).

Similar studies using a subset of the AMO designs were performed for miR-122, miR-24, and miR-16. New luciferase reporter vectors were constructed containing perfect match sites for these miRNAs in the RLuc 3′UTR and AMO activity assays were performed as before, using only the 24-hour transfection protocol. The dynamic range of these assays was lower than for miR-21 and, as such, their ability to discriminate between subtle variations in potency of different AMOs was less. Sequences of the miR-24 and miR-16 AMOs are shown in **Supplemental Figure S2A**, online. These AMOs were transfected into HeLa cells at doses ranging from 0.5 to 25 nM; results of the luciferase reporter assays are shown in **Supplemental Figure S2B**, online. For the miR-24 AMOs, the original antagomir design ("miR-24 2′OMe 3PSends") had the lowest potency of the group studied while the dual-ZEN AMOs ("miR-24 2′OMe 5′inZEN, 3′inZEN" and "miR-24 2′OMe 5′inZEN, 3′ZEN"), the DNA/LNA chimera ("miR-24 DNA/LNA PS") and the 2′OMe/LNA chimera ("miR-24 2′OMe/LNA PS") showed similar increases in potency. For the miR-16 AMOs, all of the variants showed relatively similar potency with the 2′OMe/LNA chimera ("miR-16 2′OMe/LNA PS") showing highest potency at the lower doses.

The miR-122 AMO studies were performed in the Huh-7 human hepatoma cell line, providing the opportunity to examine AMO activity in a different cell type than was used in the previous studies (HeLa). In this case, both full-length 22mer miR-122 AMOs and a series of 15mer shortened AMOs were tested; the 15mers were shortened from full-length by truncation of six residues from the 5′-end (which binds to the 3′-end of the target miRNA) and one residue from the 3′-end. This 15mer design corresponds to a DNA/LNA-PS chimera AMO (SPC3469) that was previously reported by Santaris Pharma as an optimized reagent for miR-122 knockdown and which has already been demonstrated to perform well in nonhuman primate studies.[20] Sequences are shown in **Figure 5a** and results are shown in **Figure 5b**. Within the set of full-length 22mers, the dual-ZEN modified AMOs ("2′OMe 5′inZEN, 3′inZEN" and "2′OMe 5′inZEN, 3′ZEN") exhibited similar potency to the full-length LNA chimeras ("DNA/LNA PS" and "2′OMe/LNA PS"), all of which significantly outperformed the original antagomir design ("2′OMe 3PSends"). Unlike miR-21, the miR-122 dual-ZEN modified AMOs did not show any potency difference whether the 3′-modifier was placed internally ("2′OMe 5′inZEN, 3′inZEN") vs. at the terminal position ("2′OMe 5′inZEN, 3′ZEN"). This may be due to the lower sensitivity and dynamic range of the miR-122 assay or may relate to sequence differences between miR-21 and miR-122. The negative control 22mer miR-21 AMO ("miR-21 2′OMe 5′inZEN, 3′inZEN") had no effect on the miR-122 reporter.

Within the set of truncated 15mer miR-122 AMOs, the dual-ZEN compound ("15mer 2′OMe 5′inZEN, 3′Zen") and optimized 2′OMe/LNA chimera ("2′OMe SPC3469") showed highest potency, similar to the best of the full-length AMOs. In contrast, the DNA/LNA chimera with a simple alternating modification pattern ("15mer DNA/LNA PS") and the optimized candidate therapeutic compound ("SPC3469") were less potent. It is not surprising that the optimized 15mer DNA/LNA chimera showed lower potency in this context; it was intended for use *in vivo* with naked intravenous administration where short oligonucleotides show much better uptake and performance than do longer oligonucleotides.[40] In cell culture using facilitated lipid transfection, the longer (higher T_m) AMOs were expected to have higher potency. In this context, the high potency observed for the dual-ZEN miR-122 AMO was unexpected. This effect was studied in greater detail in the miR-21 system.

a

Name	miR-122 AMO Sequences (5′–3′)[a]
miR-21 2′OMe 5′inZEN, 3′inZEN	UzC A A C A U C A G U C U G A U A A G C UzA
2′OMe	C A A A C A C C A U U G U C A C A C U C C A
2′OMe 3PSends	C*A*A*A C A C C A U U G U C A C A C U*C*C*A
2′OMe 5′inZEN, 3′inZEN	CzA A A C A C C A U U G U C A C A C U C CzA
2′OMe 5′inZEN, 3′ZEN	CzA A A C A C C A U U G U C A C A C U C C Az
DNA/LNA PS	c*A*a*a*C*a*c*C*a*t*T*g*t*C*a*c*A*c*t*C*c*a
2′OMe/LNA PS	C*A*A*A*C*A*C*C*A*U*T*G*U*C*A*C*A*C*U*C*C*A
15mer 2′OMe 5′inZEN, 3′ZEN	Czc A t t G T c a C a C t C Cz
15mer DNA/LNA PS	c*C*a*t*T*g*t*C*a*c*A*c*t*C*c
SPC3469	C*c*A*t*t*G*T*c*a*C*a*C*t*C*C
2′OMe-SPC3469	C*C*A*U*U*G*T*C*A*C*A*C*U*C*C

[a]Lowercase red = DNA; Uppercase black = 2′OMe; Uppercase black underscore = LNA; "*" = PS linkage; "z" = ZEN

b

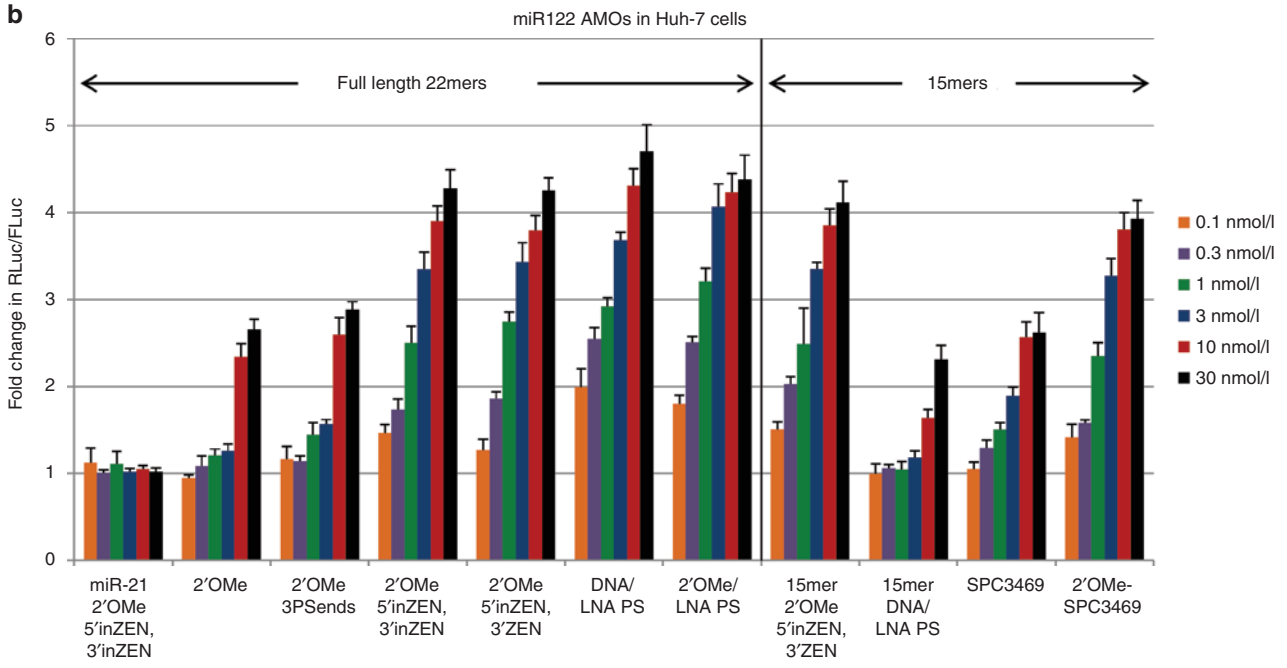

Figure 5 Potency profiles of miR-122 AMOs in Huh-7 cells. (**a**) AMOs targeting miR-122 were designed with various chemical compositions as either 22mers or 15mers. The full-length miR-21 AMO serves as a negative control. (**b**) AMOs were transfected into Huh-7 cells expressing the psiCHECK-miR-122 plasmid. Cells were lysed and analyzed for luciferase activity 24 hours post-transfection with no change in media. All values were normalized with the internal firefly luciferase (FLuc) control and reported as a fold change in *Renilla* luciferase (RLuc) compared with the lipid reagent control, which was set at 1. AMO, Anti-microRNA oligonucleotides.

A set of truncated miR-21 AMOs were compared with full-length 22mer compounds for relative potency. Truncated compounds tested included a dual-ZEN 15mer, 14mer, and 12mer and a 15mer DNA/LNA PS chimera. Melting temperatures were measured for these compounds annealed to a synthetic miR-21 RNA oligonucleotide. Sequences are shown in **Supplemental Figure S3A**, online and results are shown in **Supplemental Figure S3B**, online. The dual-ZEN 15mer ("15mer 2′OMe 5′inZEN, 3′ZEN") showed relatively high potency but was not as effective at low dose as the two full-length 22mer AMOs ("22mer 2′OMe 5′inZEN, 3′ZEN" and "22mer DNA/LNA PS"). In contrast, the 15mer dual-ZEN miR-122 AMO had equal potency to the 22mer full-length versions (**Figure 5b**). The DNA/LNA chimera ("15mer DNA/LNA PS") was less potent, inhibiting miR-21 activity only at the highest doses tested. Interestingly, function was dramatically lost as length was reduced to 14mer and 12mer length ("14mer 2′OMe 5′inZEN, 3′ZEN" and "12mer 2′OMe 5′inZEN, 3′ZEN") where the dual-ZEN AMOs showed little or no activity.

Potency grossly correlated with the measured T_m: the 22mer dual-ZEN AMO had a T_m of 76.3 °C and the less potent 15mer dual-ZEN AMO had a T_m of 69.7 °C (ΔT_m of –6.6 °C). The full length DNA/LNA PS AMO had a T_m of 74.5 °C and the less potent 15mer DNA/LNA PS AMO had a T_m of 65.7 °C (ΔT_m of –8.8 °C). It is likely that a carefully optimized 15mer

DNA/LNA PS chimera would show improved potency, similar to the miR-122 SPC3469 reagent. The inactive 14mer and 12mer dual-ZEN AMOs had T_m's of 66.3 and 57.9 °C, respectively. The 15mer DNA/LNA PS AMO had a slightly lower T_m than the 14mer dual-ZEN AMO, yet the DNA/LNA PS chimera was slightly more potent. T_m measurements typically have an expected error of ±0.5 °C. It may be that the LNA modification confers some additional advantages, which lead to higher potency beyond what is predicted by the T_m measurements. The abrupt transition seen between the 15mer and 14mer AMOs suggests that a point may exist where AMOs whose $\Delta G°$ of duplex unwinding lies above a certain threshold show good potency while those that lie below do not. Nearest-neighbor thermodynamic parameters have not been determined which permit accurate prediction of the $\Delta G°$ and T_m of a dual-ZEN AMO annealed to an RNA target. Given the widely varying GC base content (and relative binding affinities) seen between all miRNAs, it therefore seems unwise to employ short truncated AMOs like the 15mers studied here unless empiric testing and optimization is first undertaken; use of a full-length, or near full-length, AMO seems most prudent.

While it is difficult to directly compare the absolute level of change in RLuc/FLuc ratios between separate experiments, the 15mer dual-ZEN AMO appeared to have higher potency in suppressing miR-21 activity (Figure S3b) than the 22mer 2′OMe/PS chimera ("2′OMe 3PSends", **Figure 4b**), even though the full-length 2′OMe/PS chimera had a higher measured T_m (72.2, 2.5 °C higher than the more potent 15mer). This may argue for the existence of additional factors beyond nuclease stabilization and T_m increase that contribute to the improved performance of the dual-ZEN AMOs. Possibilities include more efficient invasion of miRISC, improved transfection efficiency, or alteration of intracellular distribution. The most direct method to assess transfection efficiency is to label the nucleic acid that is transfected and track signal post-transfection. Unfortunately, the ZEN modifier also functions as a dark quencher, so fluorescent tagging of these oligonucleotides will not work for this purpose. Further, having a ZEN modifier at or near the 5′-end of an oligonucleotide interferes with phosphorylation by polynucleotide kinase, so ^{32}P labeling is not an option. Instead, a series of unlabeled non-targeting negative control ("NC1") AMOs were transfected into cells and detected using *in situ* hybridization to a digoxigenin (Dig) labeled 2′OMe anti-AMO probe. Final detection was achieved using an anti-Dig antibody and an Alexa Fluor 647-conjugated secondary antibody (see "Material and Methods"). Sequences of the AMOs studied and the anti-AMO Dig-probe are shown in **Supplemental Figure S4A**, online and results are shown in **Supplemental Figure S4B**, online. The dual-ZEN AMO ("2′OMe 5′inZEN, 3′ZEN"), DNA/LNA chimera ("DNA/LNA PS"), 2′OMe/LNA chimera ("2′OMe/LNA PS") and antagomir ("2′OMe 3PSends") all had grossly similar transfection efficiencies as demonstrated by the intensity of Alexa Fluor 647-dye labeling in the *in situ* hybridization images. Curiously, the 2′OMe AMO with C3 spacers on each end ("2′OMe 5′C3, 3′C3") showed markedly lower Alexa Fluor 647 signal than the other AMOs transfected. The terminal C3 spacers block exonuclease attack, so the lower signal does not relate to nuclease stability (**Figure 2**). Further, lower signal is unlikely to be due to poor hybridization as higher signal was seen for the "2′OMe 3PSends" AMO which has a similar T_m (**Figure 3**). We therefore believe that this compound has a lower transfection efficiency than the other AMOs tested. Chemical composition of a transfected nucleic acid can affect transfection efficiency; it is possible that the greater hydrophobicity of the PS-modified AMOs as well as the ZEN modifier improves transfection, at least with certain lipids.

Optimization of ZEN-AMO design

Optimization of ZEN placement at the 3′- and 5′-ends of the AMO was studied in greater detail using the miR-21 system. To study the 3′-end, miR-21 2′OMe AMOs were synthesized with an unmodified 5′-end with the following 3′-modifications: 3′ZEN, 3′inZEN, 3′inC3, or with a terminal LNA residue and a 3′C3 modifier. The LNA residue was employed to increase T_m of the C3-modified variants to simulate the increase in binding affinity provided by the ZEN modification as one way to isolate effects that come from 3′-nuclease stabilization as opposed to those arising from increases in binding affinity. While LNA modification is traditionally associated with improved nuclease resistance, oligonucleotides remain nuclease sensitive when only a single LNA residue is incorporated at the 3′-end. For the designs studied here, a 3′-terminal blocking group (such as a C3 spacer) was required to protect 3′-LNA modified AMOs from degradation by the 3′-exonuclease activity present in serum (see **Supplemental Figure S5**, online). Serial truncations ranging from 22mer to 19mer length were compared. Melting studies were performed to determine T_m. AMO sequences and measured T_m values are shown in **Figure 6a** and results of the functional potency study are shown in **Figure 6b**. While sequence names indicate the length of the AMO as synthesized, the chart in **Figure 6b** has the sequences grouped by the expected length after exposure to serum and cellular nucleases where AMOs having a 3′inC3 or 3′inZEN loses the 3′-terminal nucleotide (**Figure 2a**, **b**).

The AMOs that survive transfection as 22mers both showed high potency ("22 3′ZEN" and "22 3′LNA,C3") while the 22mer with 3′inC3 modification, which drops to 21mer length in serum ("22 3′inC3"), showed lower potency, consistent with its lower measured T_m (ΔT_m of –2 °C) and lower transfection efficiency (**Supplemental Figure S4**, online). As anticipated from earlier results (**Figure 4b**), the most potent AMOs of this series were the 3'-ZEN-modified variants which survive serum exposure as 21mers ("22 3′inZEN" and "21 3′ZEN"); the 21mer LNA variant ("21 3′LNA,C3") was significantly less potent, in spite of having a similar T_m. A large reduction in potency was seen as the length was further reduced to a 20mer or a 19mer. The "3′inZEN,C3" AMO was protected at 22mer length by the terminal C3 modifier but in this case, the ZEN group was placed between nucleotides 19 and 20. It showed low potency, consistent with its lower T_m (ΔT_m of around –4 °C compared with "21 3′ZEN"). At least for the miR-21 system, potency correlated with a combination of high T_m and having a final 21mer AMO paired to the 22mer miR-21. This may relate more to the interaction of the AMO with the miRNA in miRISC more than the predicted T_m of the AMO with the miRNA (see later discussion).

a

Name	miR-21 AMO sequences[a]	T_m(°C)[b]
2′OMe 22 3′ZEN	U C A A C A U C A G U C U G A U A A G C U Az	74.0
2′OMe 22 3′LNA, C3	U C A A C A U C A G U C U G A U A A G C U A^	73.8
2′OMe 22 3′inC3	U C A A C A U C A G U C U G A U A A G C U^A	72.0
2′OMe 22 3′inZEN	U C A A C A U C A G U C U G A U A A G C UzA	73.4
2′OMe 21 3′ZEN	U C A A C A U C A G U C U G A U A A G C Uz	71.9
2′OMe 21 3′LNA, C3	U C A A C A U C A G U C U G A U A A G C U^	72.1
2′OMe 21 3′inZEN	U C A A C A U C A G U C U G A U A A G CzU	70.9
2′OMe 20 3′ZEN	U C A A C A U C A G U C U G A U A A G Cz	70.6
2′OMe 20 3′LNA, C3	U C A A C A U C A G U C U G A U A A G C^	70.8
2′OMe 20 3′inZEN	U C A A C A U C A G U C U G A U A A GzC	66.5
2′OMe 19 3′ZEN	U C A A C A U C A G U C U G A U A A Gz	67.3
2′OMe 19 3′LNA, C3	U C A A C A U C A G U C U G A U A A G^	67.4
2′OMe 22 3′inZEN, C3	U C A A C A U C A G U C U G A U A A GzC U A^	67.9

[a]Uppercase = 2′OMe; Uppercase underscore = LNA; "z" = ZEN; "^" = C3 spacer
[b]Duplexes were annealed in 150 mmol/l Na^+ buffer to an RNA complement.

b

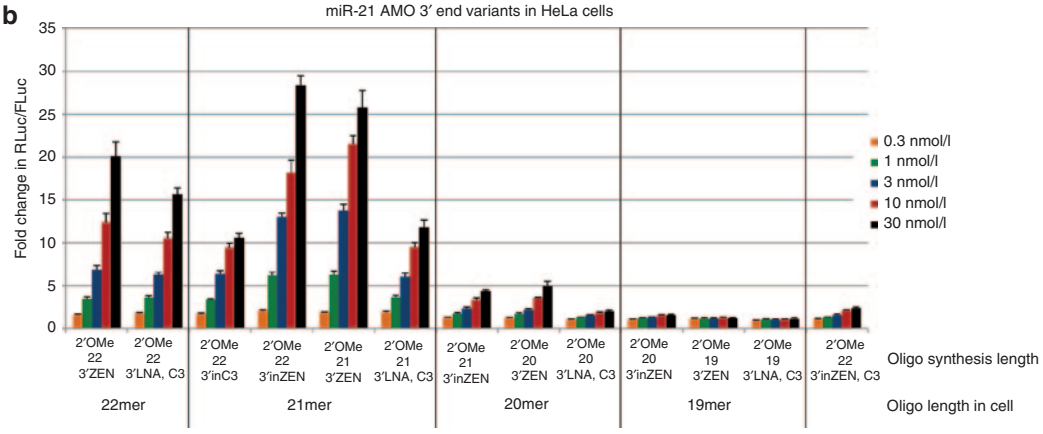

Figure 6 3′-end optimization of miR-21 AMO designs. (**a**) 2′OMe AMOs targeting miR-21 were designed with serial nucleotide truncations at the 3′-end. 3′-ends were modified with either 3′ZEN, 3′inZEN, or a terminal LNA residue with 3′C3. 5′-ends were unmodified. Measured T_m values are shown to the right. (**b**) AMOs were transfected into HeLa cells expressing the psiCHECK-miR-21 plasmid. Cells were lysed and analyzed for luciferase activity 24 hours post-transfection with no change in media. All values were normalized with the internal firefly luciferase (FLuc) control and reported as a fold change in *Renilla* luciferase (RLuc) compared with the lipid reagent control, which was set at 1. AMOs are grouped according to their final "nuclease resistant length", not their length as synthesized, to account for anticipated loss of the 3′-terminal nucleotide to 3′-exonuclease attack for the 3′inZEN designs. AMO, Anti-microRNA oligonucleotides.

A similar 3′-end optimization study was done for the miR-122 AMO. Sequences studied are shown in **Supplemental Figure S6A**, online. As before, the miR-122 AMOs were functionally studied in Huh-7 cells; results are shown in **Supplemental Figure S6B**, online. In this case, the AMOs having a final functional length of 22mer ("22 3′ZEN") and 21mer ("22 3′inZEN" and "21 3′ZEN") showed identical potency. However, as with miR-21, the activity rapidly decreased as the length of the intact AMO dropped to a 20mer or a 19mer. The reductions in potency observed here with a small number of 3′-base deletions is far more dramatic than that seen previously (**Supplemental Figure S3**, online) for larger 5′-truncations. The 3′-end of the AMO binds the miRNA seed region, which is critical to AMO function and which presumably relates to the large loss of potency seen with 3′-truncations in the AMO sequence. In addition, the compounds studied in **Supplemental Figure S3**, online were dual-ZEN modified, whereas the end optimization studies were performed using only a single-ZEN modification, to better isolate end effects.

For optimization at the 5′-end, a set of miR-21 2′OMe AMOs were synthesized having either a 5′ZEN or 5′inZEN modification with a C3 spacer modifier at the 3′-end to block exonuclease attack. Serial truncations ranging from 22mer to 19mer length were compared. In this case, length of the intact AMO following transfection is expected to be unchanged from the original oligonucleotide synthesized. AMO sequences are shown in **Figure 7a** and results of the functional potency study performed in HeLa cells are shown in **Figure 7b**. Unlike at the 3′-end, variation in the 5′-end design did not show large differences and in general functional potency slowly decreased as the AMOs were shortened. A similar 5′-end optimization study was performed for miR-122 AMOs in Huh-7 cells. Sequences are shown in **Supplemental Figure S7A**, online and functional results are shown in **Supplemental Figure S7B**, online. Like the results for the miR-21 AMOs, variations in the 5′-end did not show large differences in potency and in general functional potency just slowly decreased as the length of the AMO decreased. The aggregate of data from the study of nuclease stability, T_m, and potency indicated that the optimal design of a dual-ZEN AMO is a 2′OMe oligonucleotide with 5′inZEN and 3′ZEN modifiers using a sequence complementary to the target miRNA, deleting the 3′-terminal residue so that the AMO is one nucleotide shorter than the target miRNA.

a

Name	miR-21 AMO sequences[a]
2′OMe 22 5′ZEN/3′C3	zU C A A C A U C A G U C U G A U A A G C U A^
2′OMe 22 5′inZEN/3′C3	UzC A A C A U C A G U C U G A U A A G C U A^
2′OMe 21 5′ZEN/3′C3	zC A A C A U C A G U C U G A U A A G C U A^
2′OMe 21 5′inZEN/3′C3	CzA A C A U C A G U C U G A U A A G C U A^
2′OMe 20 5′ZEN/3′C3	zA A C A U C A G U C U G A U A A G C U A^
2′OMe 20 5′inZEN/3′C3	AzA C A U C A G U C U G A U A A G C U A^
2′OMe 19 5′ZEN/3′C3	zA C A U C A G U C U G A U A A G C U A^

[a]uppercase = 2′OMe; "z" = ZEN; "^" = C3 spacer

b

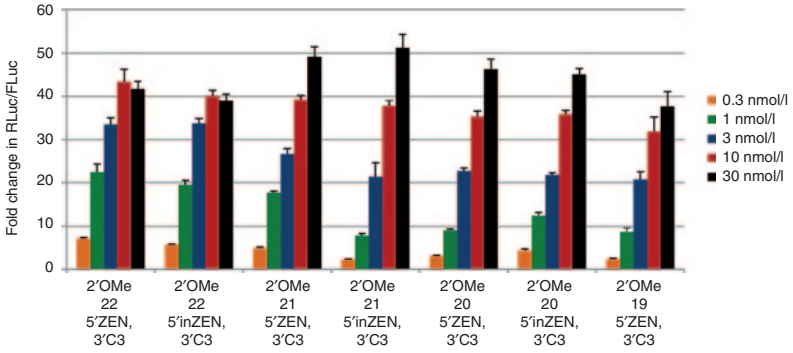

Figure 7 5′-end optimization of miR-21 AMO designs. (**a**) 2′OMe AMOs targeting miR-21 were designed with serial truncations at the 5′-end. The 5′-ends were modified with either 5′ZEN or 5′inZEN. 3′-ends were modified with a 3′C3 to block exonuclease attack. (**b**) AMOs were transfected into HeLa cells expressing the psiCHECK-miR-21 plasmid. Cells were lysed and analyzed for luciferase activity 24 hours post-transfection with no change in media. All values were normalized with the internal firefly luciferase (FLuc) control and reported as a fold change in *Renilla* luciferase (RLuc) compared with the lipid reagent control, which was set at 1. AMO, Anti-microRNA oligonucleotides.

AMO specificity

A variety of features contribute to AMO potency, with increased binding affinity to the targeted miRNA being one of the most influential factors.[6] We previously suggested that increasing binding affinity will increase potency up to some threshold level, after which gains in potency are relatively small and further increases in binding affinity only serve to increase the potential for unintended hybridization to closely related targets.[7] The original antagomir design ("2′OMe 3PSends") shows a lower T_m and lower potency than other designs tested in the present study and would be predicted to show the highest specificity. Single base discrimination has been reported using this design to suppress miR-122 in mouse livers.[16] The DNA/LNA chimeras and dual-ZEN AMOs have relatively similar T_m's and potency; however, the LNA residues are placed internally throughout the sequence while ZEN modifications are terminal, which may alter mismatch discrimination between these designs. To test whether this positional difference of the high binding affinity modifications in the LNA chimeras vs. the ZEN-AMO constructs affects specificity, mutations were placed in a series of miR-21 AMOs at one, two or three positions (**Figure 8a** and **Supplemental Figure S8**, online). Specificity of the various designs was tested using the wild type miR-21 RLuc reporter and results are shown in **Figure 8b**. The "2′OMe 5′inZEN, 3′inZEN", "2′OMe 5′inZEN, 3′ZEN" and "DNA/LNA PS" AMOs all showed similar specificity where a single mismatch could be discriminated at lower doses (3 nmol/l or less) and two mismatches were easily distinguished at all doses studied. As predicted, the "2′OMe 3PSends" AMO showed the highest specificity and loss of activity with a single mismatch; however, it also demonstrated the lowest potency. As expected, the least specific AMO in the group was the 2′OMe/LNA chimera ("2′OMe/LNA PS"), which retained activity even with two mismatches. As an alternative way of viewing the specificity data, **Supplemental Figure S9**, online shows the ratio between the activity of the mutant and perfect match at various doses, where a fold change of "1" indicates identical activity between the mismatched AMO and the perfect match AMO. The rank order of specificity of the AMO designs is: "2′OMe 3PSends" > dual-ZEN or DNA/LNA PS chimera >> 2′OMe/LNA PS chimera.

Toxicity of the different AMO designs

It is well known that synthetic oligonucleotides can have significant toxic effects when transfected into mammalian cells. Some of these effects relate to the presence of foreign nucleic acids in cells (for example, some compounds can trigger an innate immune response), some are specific to certain chemical modifications, and some relate to or are influenced by the transfection reagent. Thus, the AMOs studied here could cause toxicity through a variety of mechanisms. 2′OMe RNA is a natural nucleic acid that has no significant chemical toxicity of its own; in fact, it can block unwanted immune responses caused by RNA.[41] The well-known toxicities associated with LNA residues have already been discussed. PS linkages can cause cytotoxicity, often in an incremental progression that directly correlates with the number of PS linkages present and is worse when used with DNA than 2′-modified residues (Behlke and Lennox, unpublished observation).[26,42] ZEN is a new non-nucleotide modifying group that has not previously been studied for possible toxic effects. The relative toxicity of various AMO designs

were compared in HeLa cells using a 22mer nontargeting negative control sequence (NC1) unrelated to any known human miRNA. Sequences of the AMOs tested are shown in **Figure 9**. After verification that all oligonucleotides were free from endotoxin contamination, the AMOs were transfected at 10, 30, and 100 nmol/l concentrations using three different transfection reagents Lipofectamine RNAiMAX, INTERFERin and Lipofectamine 2000. Cells were examined visually by microscopy at 24-hour post-transfection and then were analyzed for signs of cytotoxicity (from necrosis and/or apoptosis) using a commercial assay. Treatment with 1 µmol/l staurosporine was included as a positive control for cytotoxicity. Photomicrographs showing images of the cultures at 24-hour post-transfection using Lipofectamine RNAiMAX are shown in **Figure 10**. Results obtained from testing cultures with a semi-quantitative commercial toxicity assay are shown in **Supplemental Figure S10**, online for all three transfection reagents.

Unmodified 2′OMe RNA showed no toxicity under any dose tested using all three transfection reagents. The dual-ZEN modified AMO ("2′OMe 5′inZEN, 3′ZEN") and "2′OMe/LNA PS" AMO showed normal appearing cells to visual examination (**Figure 10**) and had a slight reduction in cell viability detected for the Lipofectamine transfection reagents but not when using the INTERFERin (**Supplemental Figure S10**, online). The "2′OMe 3PSends" AMO (which is limited to six PS linkages) showed obvious cell death to visual examination with toxicity that varied with dose and which transfection reagent was employed; greatest toxicity was seen when using the Lipofectamine 2000 reagent. Two different syntheses of the NC1 "2′OMe 3PSends" oligonucleotide as well as a different negative control sequence gave the same results (data not shown). The "DNA/LNA PS" AMO showed the highest toxicity, resulting in up to 80% cell death. Interestingly, the "2′OMe/LNA PS" oligonucleotide was less toxic when compared with the "DNA/LNA PS" AMO, suggesting that substitution of 2′OMe residues for DNA might elicit some protection. This protective effect from the 2′OMe modification is not a result of evading a TLR9 innate immune response from DNA CpG motifs in the

a

Mutant type	miR-21 AMO sequences (5′–3′)[a]
Wildtype	U C A A C A U C A G U C U G A U A A G C U A
MUT 1	U C A A C A U C A G U C **A** G A U A A G C U A
MUT 2	U C A A C **C** U C A G U C **A** G A U A A G C U A
MUT 3	U C A A C **C** U C A G U C **A** G A U A A **C** C U A

[a]Mutations are notated as blue nucleotides enclosed in red boxes

b

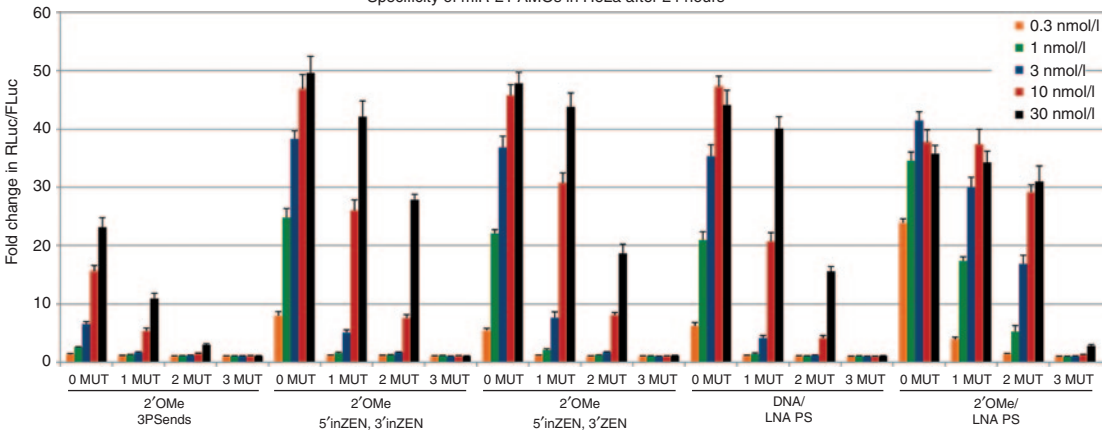

Figure 8 Specificity of miR-21 AMOs. (**a**) Five different miR-21 AMO designs were synthesized complementary to either the wild type miR-21 sequence or containing 1, 2, or 3 mismatches. (**b**) AMOs were transfected into HeLa cells expressing the psiCHECK-miR-21 plasmid. Cells were lysed and analyzed for luciferase activity 24 hours post-transfection with no change in media. All values were normalized with the internal firefly luciferase (FLuc) control and reported as a fold change in *Renilla* luciferase (RLuc) compared with the lipid reagent control, which was set at 1. AMO, Anti-microRNA oligonucleotides.

Name	NC1 AMO sequences (5′–3′)[a]
NC1 2′OMe	G C G U A U U A U A G C C G A U U A A C G A
NC1 2′OMe 3PSends	G*C*G*U A U U A U A G C C G A U U A A*C*G*A
NC1 2′OMe 5′inZEN, 3′ZEN	GzC G U A U U A U A G C C G A U U A A C G Az
NC1 DNA/LNA PS	g*C*g*t*A*t*t*A*t*a*G*c*c*G*a*t*T*a*a*C*g*a
NC1 2′OMe/LNA PS	G*C*G*U*A*U*U*A*U*A*G*C*C*G*A*U*T*A*A*C*G*A

[a]Lowercase red = DNA; Uppercase black = 2′OMe; "*" = PS linkage; "z" = ZEN insertion
Uppercase black underscore = LNA

Figure 9 Sequences of nontargeting AMOs employed in toxicity testing. A sequence that does not target any known miRNAs (NC1) was synthesized using the AMO designs shown. AMO, Anti-microRNA oligonucleotides.

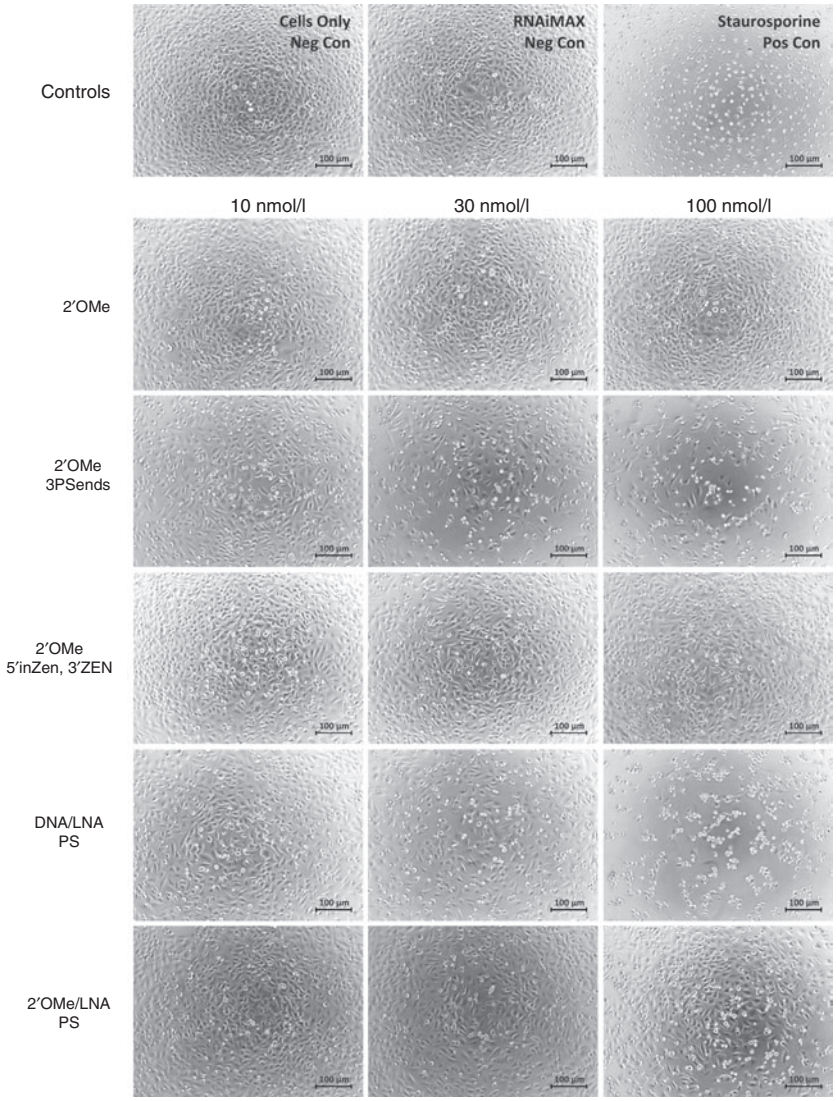

Figure 10 Toxicity testing of nontargeting AMOs in HeLa cells. The NC1 AMOs (Figure 9) were transfected into HeLa cells at 10, 30, and 100 nmol/l concentrations and visualized using phase contrast microscopy at 10× magnification. A 100-micron scale bar is indicated in each photomicrograph. Staurosporine is a positive control toxic compound. AMO, Anti-microRNA oligonucleotides.

oligonucleotide,[43] as substitution of 5-methyl-deoxycytosine for deoxycytosine in the "DNA/LNA PS" AMO does not alter toxicity of this compound (data not shown).

Discussion

This study describes a novel non-nucleotide modification (N,N-diethyl-4-(4-nitronaphthalen-1-ylazo)-phenylamine or "ZEN") that is useful in antisense applications. The present investigation was focused on improving reagents to suppress miRNA activity, but the new ZEN modifier should also be useful in other antisense applications, such as splice-switching or to suppress mRNA translation. The most significant property of the ZEN modification is that it increases the T_m of an oligonucleotide when placed either as an insertion between nucleotides or at the terminal ends of an oligonucleotide and thereby enhances the potency of the antisense compound. Interestingly, the magnitude of the T_m increase is greater when the modification is used at the 5′-end of the oligonucleotide than at the 3′-end and is additive when placed at both ends. The new compound is a planar, hydrophobic molecule that may fit between bases and contribute to base stacking interactions. Alternatively, when the ZEN group is placed at or near the end of the oligonucleotide, it may contribute to stacking interactions by capping the end of the duplex. Future studies will include NMR and/or X-ray crystallography to better understand the mechanisms at work, which may suggest ways to modify the compound to improve this effect.

ZEN, like most non-nucleotide modifiers, can block exonuclease attack when incorporated at the 5′- and 3′-ends of the oligonucleotide. This property, combined with the boost in binding affinity, enables use of the ZEN modifier with a simple 2′OMe RNA oligonucleotide backbone without the need for other T_m-enhancing modifications, such as LNA residues, or nuclease resistant modifications, such as PS linkages, thereby avoiding their associated toxicities. In addition, the ZEN

Table 1 A comparative analysis of desired AMO characteristics

AMO	Nuclease stability	T_m	Potency	Specificity	Toxicity	Mixture of diastereomers
2′OMe	+	-	+	ND	-	None
2′OMe, 5′inZEN, 3′ZEN	++++	↑↑	+++	+++	+/-	None
2′OMe 3PSends	+++	↓	++	++++	++	++
DNA/LNA PS	+++	↑↑	+++	+++	+++	++++
2′OMe/LNA PS	+++	↑↑↑↑	++++	+	+	++++

AMO, Anti-microRNA oligonucleotides.
The effectiveness of the modification pattern on a given characteristic is scored as follows: +, relative level, with "+", low and "++++", high; -, baseline value; "↑" = an increase in value; "↓" = a decrease in value.
ND, not determined.

modification does not introduce a new chiral center into the molecule, avoiding the complication of having a mixture of diasteriomers present. **Table 1** provides a summary of the various features of the different AMOs compared in the present study. While all of the AMOs studied showed good stability against degradation in serum or cell extract, the "2′OMe 5′inZEN, 3′ZEN" AMOs were unique in that they were completely resistant to both endo- and exonuclease attack. The "2′OMe/LNA PS" AMO by far had the highest T_m of all of the compounds, was the most potent, and was fairly nontoxic; however, it had the lowest specificity. The "DNA/LNA PS" AMO had a high T_m, was potent and showed good specificity; however, this AMO construct had high toxicity, even when used with HeLa cells (a fairly robust cell line). The "2′OMe 3PSends" AMO had the highest specificity of the group, but, with its lower T_m, showed the lowest potency and surprisingly also had some degree of toxicity. The dual-ZEN modified "2′OMe 5′inZEN, 3′ZEN" AMO had the best combination of properties, including a high T_m, high potency, good specificity, and low toxicity.

The 3′ end of an AMO is an important determinant of AMO functionality as it binds to the miRNA seed region (the most critical miRNA domain, spanning from bases 2–8 on the 5′ end). AMOs are usually designed to be full length, perfect match complements to the target miRNA, unless potent T_m-enhancing modifications like LNAs are employed. Without the use of T_m-enhancing modifications, truncation of an AMO lowers the binding affinity to the target and results in reduced potency. One notable exception to this rule is that deletion of the 3′-terminal nucleotide in the dual-ZEN AMOs showed increased potency against the miR-21 target (or resulted in no change in potency for the miR-122 target); in no case tested has this decreased potency. This intriguing result may be explained by how the miRNA associates with the AGO2 protein in miRISC. The 5′ terminal nucleotide of the miRNA (complementary to the 3′-end of the AMO) is embedded in a deep pocket in between the MID and PIWI domains of AGO2[44] and is not available for hybridization to the AMO. Presumably, the ZEN modification requires interaction with the miRNA to increase binding affinity, so having the ZEN positioned opposite of residue #2 of the miRNA may result in a more energetically favorable interaction than when it is aligned with the 5′-terminal nucleotide of the miRNA, which is bent away from the AMO. This is consistent with results from a previous study, which also described benefits from a single nucleotide truncation at the 3′-end of an AMO.[17]

The most potent AMO, the 2′OMe/LNA chimera ("2′OMe/LNA PS") had the lowest specificity and suppressed miR-21 activity even when two mismatches were present. This design would be appropriate to use if it was desired to suppress multiple related species, such as targeting an entire miRNA family. It was recently reported that short 8mer LNA-PS oligonucleotides, which bind to the miRNA seed region, could be used to inhibit entire families of miRNAs.[45] It would be interesting to test if addition of the ZEN modification to the tiny LNA AMOs results in increased potency.

A large increase in potency was observed with the addition of the ZEN modifiers ("2′OMe 5′inZEN, 3′ZEN") or LNA residues ("DNA/LNA PS") compared with the "2′OMe 3PSends" AMO, yet the T_m only increased by 2–4 °C. In contrast, the "2′OMe/LNA PS" AMO showed only a modest increase in potency over the dual-ZEN AMOs in spite of an additional increase in T_m of 11 °C (**Figure 4**). Further, the miR-21 dual-ZEN AMO truncation experiment (**Supplemental Figure S3**, online) showed a sharp transition between 15 and 14 base lengths, where efficacy was suddenly lost. These observations are consistent with the idea that a threshold binding affinity exists and reagents with a $\Delta G°$ change above this level work well and those with a $\Delta G°$ below this level do not. We speculate that this threshold $\Delta G°$ identifies a point where the AMO:miRNA duplex can no longer be unwound by the helicase activity present in miRISC (which is responsible for separating the passenger and guide strands). Once this required level of stability has been achieved, further increases in binding affinity simply serve to reduce specificity without compensatory gains in potency.[7] Davis *et al.*[17] observed that a good AMO makes a poor siRNA passenger strand: it cannot be degraded by Ago2 or unwound by RISC helicase. We found that the dual-ZEN AMO design indeed made a poor passenger strand and siRNAs made using this modification pattern are inactive (data not shown).

Toxicity from chemical modification of synthetic oligonucleotides can confound data interpretation, especially if the knockdown target is itself involved in cell viability. Cells transfected with the dual-ZEN AMOs appeared normal and healthy to visual inspection with little evidence for toxicity when transfected using a variety of cationic lipids into HeLa cells, even at high concentrations of AMO (100 nmol/l). Clear evidence for toxicity was observed with both PS and LNA modifications, especially when used in combination with DNAs, and varied with different lipid transfection reagents. INTERFERin showed the least adverse effects when using LNA or PS modifications. Much higher potency was seen if the AMO/lipid complex was left on the cells for 24 hours rather than 6 hours and use of this

Figure 11 Preferred design of ZEN-AMOs. The preferred design of ZEN-AMOs for use *in vitro* is shown with the mature target miRNA on top (5′ to 3′) and the dual-ZEN AMO aligned below (3′–5′). M, 2′OMe RNA, R, RNA, p, phosphate, and z, ZEN modifier. The miRNA seed region (bases 2–8) is indicated. AMO, Anti-microRNA oligonucleotides.

protocol is recommended if the cell line employed can tolerate prolonged exposure to lipids and AMOs without toxic side effects.

Although efficacy was demonstrated for dual-ZEN AMOs as short as 15mers (**Figure 5** and **Supplemental Figure S3**, online), this length is borderline to the threshold where function is lost, at least for miR-21. Shorter length may be tolerated for miRNAs with higher GC content. However, in the absence of empiric testing or the ability to predict the T_m of a 2′OMe-ZEN oligonucleotide duplexed with an RNA target, it seems prudent to routinely make the dual-ZEN AMOs at or near full length for the target miRNA. We sometimes observed increased potency if the dual-ZEN AMO was truncated from full length by one base from the 3′-end; we have not yet observed any loss of potency from this short deletion. We therefore recommend that dual-ZEN AMOs be designed as (*N*–1)mer from perfect complementarity to the target miRNA, deleting the 3′-terminal residue (leaving the 5′-terminal base of the miRNA unpaired), as schematically shown in **Figure 11**. This approach should ensure high potency regardless of GC-content of the target miRNA.

In vivo testing of the dual-ZEN AMOs is in progress. Preliminary experiments indicate that no obvious toxicity results from direct IV injection of ZEN-modified oligonucleotides into mice (data not shown). Historical experience using antisense oligonucleotides with naked IV injection suggests that PS modification of the antisense oligonucleotide facilitates cell uptake and improves pharmacodynamics through increased binding to serum proteins (primarily albumin), increasing serum half-life and decreasing the rate of urinary excretion.[29,42] We find that PS modification of the dual-ZEN AMOs lowers binding affinity and lowers potency *in vitro*. Short antisense oligonucleotides (such as 12–14mers) penetrate tissues and enter cells with higher efficiency than long antisense oligonucleotides (such as 20mers).[40] These observations argue against use of full-length (phosphodiester) dual-ZEN AMOs *in vivo* without a delivery vehicle. It may be possible through use of additional T_m-enhancing modifications that a variant dual-ZEN AMO may tolerate PS modification and retain potency when extensively truncated. The first *in vivo* experiments using dual-ZEN AMOs, however, will employ the current optimized design (**Figure 11**) complexed with a delivery vehicle that permits *in vivo* administration of phosphodiester oligonucleotides that are >20mer length.

Materials and methods

Oligonucleotide synthesis and quantification. All oligonucleotides employed in this study were synthesized using standard phosphoramidite chemistry, purified by RP-HPLC and used in sodium salt form (Integrated DNA Technologies, Coralville, IA). The predicted masses for the oligonucleotides were verified by electrospray-ionization mass spectrometry (ESI-MS) and were within ±0.02%, and capillary electrophoresis analysis confirmed all had >90% purity. The oligonucleotide concentrations were determined from UV absorbance at 260 nm and estimated extinction coefficients.[46] LNA, 2′-*O*-methyl RNA and phosphorothioate modifications were assumed to have negligible effect on the extinction coefficient. Each ZEN modification increased the oligonucleotide extinction coefficient by 13,340 l/(mol cm). Oligomer concentrations for the UV melting experiments were measured at 85 °C and were estimated twice for each sample using different dilution factors. The measurements were discarded and repeated if the concentrations differed by more than 4%.

UV melting experiments. The AMO duplex samples were melted in a buffer containing 131 mmol/l NaCl, 10 mmol/l sodium phosphate, 1 mmol/l Na_2EDTA (total $[Na^+]$ = 150 mmol/l). A similar buffer was used for the 10mer DNA duplexes, but NaCl concentration was 1 mol/l. The pH was adjusted to 7.0 using 1 mol/l NaOH. Chemicals of p.a. or better purity were obtained from Thermo Fisher Scientific (Pittsburg, PA, USA). Stock solutions of the single strand oligomers were dialyzed against an IDT TE buffer solution (Integrated DNA Technologies, Coralville, IA, USA) containing 10 mmol/l Tris and 0.1 mmol/l EDTA (pH = 7.5) for at least 24 hours. Molecular weight cutoff of Spectra/Por 7 dialysis membrane (Spectrum Laboratories, Rancho Dominguez, CA, USA) was 1,000. The complementary anti-miRNA oligonucleotides were mixed with a synthetic miR-21 RNA (5′ pUAGCUUAUCAGACUGAUGUUGA where all nucleotides are RNA and "p" denotes a phosphate) in 1:1 molar ratios, heated to 95 °C for 2 minutes, and slowly cooled to room temperature for 20 minutes.

Methods and analyses of melting experiments were previously published.[47,48] Optical melting experiments were conducted using a single-beam Beckman DU 650 spectrophotometer with a Micro Tm Analysis accessory, a Beckman High Performance Peltier controller, and a 1 cm path-length cuvette (Beckman Coulter, Fullerton, CA, USA). Absorbance values at 268 nm as a function of temperature were acquired every 0.1 °C in the temperature range of 10–98 °C. Duplexes were melted at a total single strand concentration (C_t) of 2 µmol/l. Heating (denaturation) and cooling (annealing) transition curves were recorded at a constant temperature change rate of 25 °C/hour. Six to eight melting curves were collected for each duplex in different cuvettes. The absorbance values of the buffer melting curves were subtracted from the duplex melting curves. The melting curves were corrected for linear sloping baselines[47,48] and smoothed by a digital filter. The T_m values were defined[47,48] as temperatures where the fraction of melted base pairs (θ) is equal to 0.5. Average standard deviation of melting temperatures was 0.6 °C. Heating and cooling melting curves were superimposable indicating that reaction conditions close to equilibrium were achieved for all duplex samples. Enthalpy and free energy changes of melting transition were estimated from derivative profiles,[38,49]

$$\Delta H^{\circ} = -6RT_m^2\left(\frac{d\theta}{dT}\right)_{T=T_m}$$

$$\Delta G^{\circ}_{37} = \Delta H^{\circ} - (37+273.15)\left[\frac{\Delta H^{\circ}}{T_m} - R\ln\left(\frac{C_t}{4}\right)\right]$$

where R is the ideal gas constant. This approach assumes that transition enthalpies and entropies are temperature-independent and melting transitions proceed in two-state manner.[38]

Serum stability assay. A male mouse was sacrificed via cervical dislocation followed by immediate dissection of the liver as previously described.[6] Briefly, 1 g of liver tissue was placed into 10 ml of T-PER tissue protein extraction reagent (Pierce, Rockford, IL, USA) containing a 1 out of 100 volume cocktail of protease inhibitors (Sigma–Aldrich, St. Louis, MO, USA). The liver-extraction reagent mixture was homogenized at 35,000 RPMs for 1 min using a 10 mm stainless steel probe on an Omni TH homogenizer (Omni International, Kennesaw, GA), followed by centrifugation at 10,000×*g* for 5 min. The supernatant was stored at –80 °C.

The AMOs were diluted to 15 µmol/l in phosphate buffered saline (PBS) in a 70 µl total reaction volume and incubated in 10 and 50% nonheat-inactivated FBS (Life Technologies, Grand Island, NY, USA), or 20 and 50% mouse liver protein extract at 37 °C for 0, 2, 6, 24 or 96 hours. Degradation reactions were stopped at each time point by adding an equal volume of 2× formamide gel loading buffer (90% formamide, 1× TBE, 0.025% w/v bromophenol blue, and 0.025% w/v xylene cyanol) and immediately flash freezing on dry ice with –80 °C storage. Two hundred picomoles (13.33 µl) of each reaction was heated to 95 °C for 5 min and placed on ice for 2 minutes, loaded on 7 mol/l urea 20% polyacrylamide gels and electrophoresed at 30 mA. Gels were stained for 30 minutes in a methylene blue solution (0.02% w/v methylene blue in 0.1× TBE), destained in several washes of H_2O for 2 hours and images were generated with an HP Scanjet 4850 Photo Scanner (Hewlett-Packard Company, Palo Alto, CA).

ESI-LC-MS analysis of AMO degradation products. A 15 µl (225 pmoles) aliquot of each degradation reaction in both 10% FBS and 20% mouse liver protein extract at the 24-hour time point was analyzed by electrospray-ionization liquid chromatography mass spectrometry (ESI-LC-MS) for evaluation of degradation products. The 20% mouse liver protein extract reactions were incubated with 200 µg/ml of Proteinase K (Sigma–Aldrich) at 37 °C for 1 hour. The 10% FBS and Proteinase K-digested 20% mouse liver protein extract treated AMOs were extracted with an equal volume of Phenol:Chloroform:Isoamyl Alcohol 25:24:1 (Sigma–Aldrich) and ethanol precipitated (3 µl of 10 µg/µl glycogen, 1/10 vol 3 mol/l Na+ acetate pH 5.2, 2.5 vol cold EtOH). Pellets were re-suspended in 60 µl H_2O and the entire sample was analyzed by ESI-LC-MS using an Oligo HTCS system (Novatia, Princeton, NJ, USA)[50] consisting of a ThermoElectron LTQ, Xcalibur data system, ProMass data processing software and Paradigm MS4_HPLC (Michrom BioResources, Auburn, CA, USA).

Plasmid preparation. The plasmids were prepared as previously described.[6] The sequences used to generate the duplexes with Xho1 and Not1 overhangs for cloning into the psiCHECK-2 vector (Promega, Madison, WI) are as follows, where the italicized sequence indicates the miRNA binding domain: one perfect match miR-21 binding site (5′-pTCGAGCGAGCCGGTC*TCAAC ATCAGTCTGATAAGCTA*CCGGATCGCGGGCTGC-3′, 5′-pGGCCGCAGCCCGCGATCCGGTAGCTTATCAGACTG ATGTTGAGACCGGCTCGC-3′), one perfect match miR-122 binding site (5′-pTCGAGCGAGCCGGTC*CAAACACCATTG TCACACTCCA*CCGGATCGCGGGCTGC-3′, 5′-pGGCCGCA GCCCGCGATCCGGUGGAGTGTGACAATGGTGTTTGGA CCGGCTCGC-3′), one perfect match miR-24 binding site (5′-pTCGAGCGAGCCGGTC*CTGTTCCTGCTGAACTG AGCCA*CCGGATCGCGGGCTGC-3′, 5′-pGGCCGCAGCCC GCGATCCGGTGGCTCAGTTCAGCAGGAACAGGACC GGCTCGC-3′), one perfect match miR-16 binding site (5′-pT C G A G C G A G C C G G T C *C G C C A A T A T T T A C G T G C T GCTA*CCGGATCGCGGGCTGC-3′, 5′- GGCCGCAGCCCGC GATCCGGTAGCAGCACGTAAATATTGGCGGACCGG CTCGC-3′) or an arbitrary scrambled control (5′-pTCGA GCGAGCCGGTCAAGCCAGACTTTGTTGGATTTG AAATTCCGGATCGCGGGCTGC-3′, 5′-pGGCCGCAGCCC GCGATCCGGAATTTCAAATCCAACAAAGTCTGGCTTGA CCGGCTCGC-3′) where "p" denotes a phosphate. The respective single strands were annealed in 1× STE buffer (10 mmol/l Tris-HCl pH 8.0, 1 mmol/l EDTA pH 8.0 and 100 mmol/l NaCl) by heating to 95°C for 2 min and ligated into the Xho1/Not1 sites in the psiCHECK-2 vector with T4 DNA ligase (New England Biolabs, Ipswich, MA, USA). Ligation reactions were transformed into One Shot TOP10 Chemically Competent *E. coli* (Life Technologies) and plasmids were prepared with the Wizard *Plus* SV Minipreps DNA Purification System (Promega). The engineered plasmids were sequence verified, endotoxins were removed with the MiraCLEAN Endotoxin Removal Kit (Mirus Bio LLC, Madison, WI, USA) and the plasmids were filtered through a 0.2 µm filter. Plasmid concentration was measured by ultraviolet spectroscopy at 260 nm.

Cell culture and transfections. HeLa or Huh-7 cells were cultured with recommended media conditions. For transfections, both cells types were plated in 100 mm dishes in Dulbecco's Modified Essential Medium (DMEM) containing 10% FBS (Life Technologies). After the cells were 90% confluent, 5 µg of the psiCHECK-miRNA plasmid was transfected for 6 hours using Lipofectamine 2000 (Life Technologies) according to the recommended protocol. Plasmid-transfected cells were re-plated into 48-well plates at a cell density which reached ~70% cell confluency the following morning. Twenty four hours post-transfection of the plasmid, the AMOs were transfected in triplicate with 1 µl Lipofectamine RNAiMAX (Life Technologies) per well, either in serum-free media changed after 6 hours to complete media, or in DMEM with 10% FBS with no media change, according to recommended guidelines. AMO transfections were complete after 24 hours.

Luciferase assays. The cells transfected with the AMOs were lysed and firefly and *Renilla* luciferase activities were sequentially measured with the Dual Luciferase Reporter Assay System (Promega, Madison, WI, USA). A modified protocol was employed using 50 µl each of the Luciferase Assay Reagent II and Stop & Glo Reagent per reaction in a 96-well white-bottomed plate (E&K Scientific Products, Inc., Santa Clara, CA, USA). *Renilla* luciferase was measured as a fold change in expression compared with the Lipofectamine RNAiMAX reagent-only negative controls which were set at 100%. Values for *Renilla* luciferase luminescence were normalized to levels concurrently measured for firefly luciferase, which is present as a separate expression unit on the same plasmids as an internal control (RLuc/FLuc ratio).

In situ *hybridization studies.* HeLa cells were plated in 24-well plates onto circular 12 mm diameter *Coverglass for Growth* Coverglass (Fisher Scientific, Pittsburgh, PA, USA) in DMEM containing 10% FBS at a density which reached 90% confluency the following morning. Negative control (NC1) AMOs were transfected at 30 nmol/l with 2.5 µl Lipofectamine RNAiMAX or 1.25 µl Lipofectamine 2000 (Life Technologies) in a total of 500 µl volume per well in DMEM containing 10% FBS for 24 hours. Cultured cells were washed with PBS at 37 °C and fixed at room temperature for 1 hour in 2% (w/v) formaldehyde, 5% (v/v) acetic acid, and 0.9% (w/v) NaCl. Fixed cells were washed with PBS, treated with 0.2% Triton X-100 for 10 min at room temperature to increase membrane permeability, and washed again with PBS. A Dig-labeled 2′OMe probe complementary to the NC1 AMO (see **Supplementary Figure S4A**) was heat-denatured at 95 °C for 1 minute and 100 nmol/l final concentration was added to a hybridization solution (60% deionized formamide, 300 mmol/l NaCl, 30 mmol/l sodium citrate, 10 mmol/l EDTA, 25 mmol/l NaH_2PO_4, 5% dextran sulfate, and 250 ng/ml sheared salmon sperm DNA). The fixed, permeable cells were treated with this hybridization solution for >16 hours at 37 °C in a moist chamber. Following hybridization, the cells were washed twice at room temperature with a wash buffer containing 2× SSC, 300 mmol/l NaCl and 30 mmol/l sodium citrate. A second wash buffer containing 60% formamide in 2× SSC was used to wash the cells three-times at room temperature and once at 37 °C, followed by a 5 minute wash with PBS. Cells were incubated with a blocking solution (1% bovine serum albumin in PBS) to mitigate nonspecific antibody binding for 1 hour at 37 °C. Cells were washed three-times in PBS and then incubated with 0.8 µg/ml of an anti-Digoxigenin mouse IgG1κ antibody (Roche Applied Science, Indianapolis, IN, USA) in blocking solution at room temperature for 1 hour. Cells were washed three-times for 5 minutes each wash in PBS, and then incubated with a 0.8 µg/ml of an Alexa Fluor 647-labeled goat antimouse IgG (H+L) secondary antibody (Life Technologies) in blocking solution for 1 hour at room temperature. Cells were washed three-times with PBS for 5 minutes each wash. Cells were stained for 5 minutes with 300 nmol/l DAPI (4′,6-diamidino-2-phenylindole, dihydrochloride) (Life Technologies) in PBS and washed multiple times with PBS. Coverslips were inverted onto 10 µl PBS on glass slides and photomicrographs were taken at 20× magnification with confocal or fluorescent imaging using an Olympus IX51 inverted microscope equipped with an X-Cite 120 fluorescence imaging system (Olympus Corporation of the Americas, Center Valley, PA). The AMO:Dig probe was detected using the Cy5 channel, followed by DAPI detection using the UV channel.

Toxicity assays. HeLa cells were plated in 96-well plates in DMEM containing 10% FBS (Life Technologies) at a density which reached 90% confluency the following day. Negative control (NC1) AMOs were tested for endotoxin contamination using the Endosafe-PTS Endotoxin Reader (Charles River, Charleston, SC, USA) according to manufacturer's recommendations and were filtered through a 0.2 µm Acrodisc Syringe Filter with HT Tuffryn Membrane (VWR International, Radnor, PA, USA). Sterile NC1 AMOs were transfected at 100, 30, or 10 nmol/l concentrations in triplicate wells with 1 µl INTERFERin (Polyplus-transfection Inc., New York, NY, USA), Lipofectamine RNAiMAX or Lipofectamine 2000 (Life Technologies) per well in DMEM containing 10% FBS. For a positive control, staurosporine (1 mmol/l in DMSO) (Sigma–Aldrich), a known apoptosis-inducing agent, was applied at 1 µmol/l to the HeLa cells in triplicate for 24 hours. After 24 hrs of NC1 AMO treatment, the cells were analyzed for viability using the MultiTox-Glo Multiplex Cytotoxicity Assay (Promega) with the peptide-substrate GF-AFC (glycyl-phenylalanylaminofluorocoumarin), which generates a fluorescence signal upon cleavage by a "live-cell" specific protease, measured at 405 nm_{Ex}/505 nm_{Em} in a SpectraFluor Microplate Reader (Tecan Group Ltd, Männedorf, Switzerland). The same cells were subsequently analyzed for cytotoxicity by detecting a "dead-cell" protease activity in a luciferase-based assay measured on a GloMax 96 Microplate Luminometer (Promega) per manufacturer's recommendations. Cytotoxicity was visualized with phase contrast microscopy and photomicrograph images were taken at 10× magnification.

Supplementary material

Figure S1. Long-term degradation studies of ZEN AMOs.
Figure S2. Potency profiles of miR-24 and miR-16 AMOs in HeLa cells.
Figure S3. Potency comparison of shorter miR-21 AMOs in HeLa cells.
Figure S4. Use of *In Situ* Hybridization (ISH) to asses relative transfection efficiency.
Figure S5. Degradation studies of 3'-terminal LNA-modified AMOs.
Figure S6. Potency comparison of miR-122 AMO 3′-end variants.
Figure S7. Potency comparison of miR-122 AMO 5′-end variants.
Figure S8. Sequences of the wild type and mutant miR-21 AMOs used to study specificity.
Figure S9. Specificity of different miR-21 AMOs in HeLa cells.
Figure S10. Cytotoxicity of various AMO designs in HeLa cells.
Table S1. T_m of 10mer DNA Duplexes with ZEN and C3 spacer modifiers.
Table S2. ESI-MS Evaluation of AMO degradation products after 24 hrs in 10% FBS.
Table S3. ESI-MS Evaluation of AMO degradation products after 24 hrs in 20% liver protein extract.

Acknowledgments. This work was supported by grants from the National Institutes of Health awarded to M.A.B., 2R44GM085863-02 and 5R44GM085863-03. This research and open access page charges were also supported by funding from Integrated DNA Technologies, Inc.

Conflict of interest. Patent applications have been filed relating to the technologies described herein which are assigned to Integrated DNA Technologies, Inc., (IDT). JAW is both a shareholder and employee of IDT, which offers oligonucleotides and reagents for sale similar to some of the compounds described in this manuscript. All other authors are employed by IDT but do not personally own any shares or equity in IDT. IDT is not a publicly traded company.

1. Carthew, RW and Sontheimer, EJ (2009). Origins and Mechanisms of miRNAs and siRNAs. *Cell* **136**: 642–655.
2. Mann, M, Barad, O, Agami, R, Geiger, B and Hornstein, E (2010). miRNA-based mechanism for the commitment of multipotent progenitors to a single cellular fate. *Proc Natl Acad Sci USA* **107**: 15804–15809.
3. Hornstein, E (2010). miRNA activity directs stem cell commitment to a particular fate. *Cell Cycle* **9**: 4041–4042.
4. Stenvang, J, Petri, A, Lindow, M, Obad, S and Kauppinen, S (2012). Inhibition of microRNA function by antimiR oligonucleotides. *Silence* **3**: 1.
5. Bauman, J, Jearawiriyapaisarn, N and Kole, R (2009). Therapeutic potential of splice-switching oligonucleotides. *Oligonucleotides* **19**: 1–13.
6. Lennox, KA and Behlke, MA (2010). A direct comparison of anti-microRNA oligonucleotide potency. *Pharm Res* **27**: 1788–1799.
7. Lennox, KA and Behlke, MA (2011). Chemical modification and design of anti-miRNA oligonucleotides. *Gene Ther* **18**: 1111–1120.
8. Freier, SM and Altmann, KH (1997). The ups and downs of nucleic acid duplex stability: structure-stability studies on chemically-modified DNA:RNA duplexes. *Nucleic Acids Res* **25**: 4429–4443.
9. Lennox, KA, Sabel, JL, Johnson, MJ, Moreira, BG, Fletcher, CA, Rose, SD *et al.* (2006). Characterization of modified antisense oligonucleotides in Xenopus laevis embryos. *Oligonucleotides* **16**: 26–42.
10. Wagner, RW, Matteucci, MD, Lewis, JG, Gutierrez, AJ, Moulds, C and Froehler, BC (1993). Antisense gene inhibition by oligonucleotides containing C-5 propyne pyrimidines. *Science* **260**: 1510–1513.
11. Shen, L, Siwkowski, A, Wancewicz, EV, Lesnik, E, Butler, M, Witchell, D *et al.* (2003). Evaluation of C-5 propynyl pyrimidine-containing oligonucleotides *in vitro* and in vivo. *Antisense Nucleic Acid Drug Dev* **13**: 129–142.
12. Stanton, R, Sciabola, S, Salatto, C, Weng, Y, Moshinsky, D, Little, J *et al.* (2012). Chemical modification study of antisense gapmers. *Nucleic Acid Ther* **22**: 344–359.
13. Tang, JY, Temsamani, J and Agrawal, S (1993). Self-stabilized antisense oligodeoxynucleotide phosphorothioates: properties and anti-HIV activity. *Nucleic Acids Res* **21**: 2729–2735.
14. Vermeulen, A, Robertson, B, Dalby, AB, Marshall, WS, Karpilow, J, Leake, D *et al.* (2007). Double-stranded regions are essential design components of potent inhibitors of RISC function. *RNA* **13**: 723–730.
15. Krützfeldt, J, Rajewsky, N, Braich, R, Rajeev, KG, Tuschl, T, Manoharan, M *et al.* (2005). Silencing of microRNAs *in vivo* with 'antagomirs'. *Nature* **438**: 685–689.
16. Krützfeldt, J, Kuwajima, S, Braich, R, Rajeev, KG, Pena, J, Tuschl, T *et al.* (2007). Specificity, duplex degradation and subcellular localization of antagomirs. *Nucleic Acids Res* **35**: 2885–2892.
17. Davis, S, Lollo, B, Freier, S and Esau, C (2006). Improved targeting of miRNA with antisense oligonucleotides. *Nucleic Acids Res* **34**: 2294–2304.
18. Davis, S, Propp, S, Freier, SM, Jones, LE, Serra, MJ, Kinberger, G *et al.* (2009). Potent inhibition of microRNA *in vivo* without degradation. *Nucleic Acids Res* **37**: 70–77.
19. Rayner, KJ, Esau, CC, Hussain, FN, McDaniel, AL, Marshall, SM, van Gils, JM *et al.* (2011). Inhibition of miR-33a/b in non-human primates raises plasma HDL and lowers VLDL triglycerides. *Nature* **478**: 404–407.
20. Elmén, J, Lindow, M, Schütz, S, Lawrence, M, Petri, A, Obad, S *et al.* (2008). LNA-mediated microRNA silencing in non-human primates. *Nature* **452**: 896–899.
21. Elmén, J, Lindow, M, Silahtaroglu, A, Bak, M, Christensen, M, Lind-Thomsen, A *et al.* (2008). Antagonism of microRNA-122 in mice by systemically administered LNA-antimiR leads to up-regulation of a large set of predicted target mRNAs in the liver. *Nucleic Acids Res* **36**: 1153–1162.
22. Worm, J, Stenvang, J, Petri, A, Frederiksen, KS, Obad, S, Elmén, J *et al.* (2009). Silencing of microRNA-155 in mice during acute inflammatory response leads to derepression of c/ebp Beta and down-regulation of G-CSF. *Nucleic Acids Res* **37**: 5784–5792.
23. Fabani, MM and Gait, MJ (2008). miR-122 targeting with LNA/2'-O-methyl oligonucleotide mixmers, peptide nucleic acids (PNA), and PNA-peptide conjugates. *RNA* **14**: 336–346.
24. Swayze, EE, Siwkowski, AM, Wancewicz, EV, Migawa, MT, Wyrzykiewicz, TK, Hung, G *et al.* (2007). Antisense oligonucleotides containing locked nucleic acid improve potency but cause significant hepatotoxicity in animals. *Nucleic Acids Res* **35**: 687–700.
25. Hildebrandt-Eriksen, ES, Aarup, V, Persson, R, Hansen, HF, Munk, ME and Ørum, H (2012). A locked nucleic acid oligonucleotide targeting microRNA 122 is well-tolerated in cynomolgus monkeys. *Nucleic Acid Ther* **22**: 152–161.
26. Krieg, AM and Stein, CA (1995). Phosphorothioate oligodeoxynucleotides: antisense or anti-protein? *Antisense Res Dev* **5**: 241.
27. Stivers, JT and Nagarajan, R (2006). Probing enzyme phosphoester interactions by combining mutagenesis and chemical modification of phosphate ester oxygens. *Chem Rev* **106**: 3443–3467.
28. Winkler, J, Stessl, M, Amartey, J and Noe, CR (2010). Off-target effects related to the phosphorothioate modification of nucleic acids. *ChemMedChem* **5**: 1344–1352.
29. Geary, RS, Watanabe, TA, Truong, L, Freier, S, Lesnik, EA, Sioufi, NB *et al.* (2001). Pharmacokinetic properties of 2'-O-(2-methoxyethyl)-modified oligonucleotide analogs in rats. *J Pharmacol Exp Ther* **296**: 890–897.
30. Cazenave, C, Stein, CA, Loreau, N, Thuong, NT, Neckers, LM, Subasinghe, C *et al.* (1989). Comparative inhibition of rabbit globin mRNA translation by modified antisense oligodeoxynucleotides. *Nucleic Acids Res* **17**: 4255–4273.
31. De Mesmaeker, A, Altmann, KH, Waldner, A and Wendeborn, S (1995). Backbone modifications in oligonucleotides and peptide nucleic acid systems. *Curr Opin Struct Biol* **5**: 343–355.
32. Rose, SD, Behlke, MA, Owczarzy, R, Walder, JA, Thomas, DM and Marvin, MR (2011). *Methods for enhancing nucleic acid hybridization.* USPTO, UA 2011/0236898 A1.
33. Eder, PS, DeVine, RJ, Dagle, JM and Walder, JA (1991). Substrate specificity and kinetics of degradation of antisense oligonucleotides by a 3' exonuclease in plasma. *Antisense Res Dev* **1**: 141–151.
34. Eckstein, F (1983). Phosphorothioate analogues of nucleotides - tools for the investigation of biochemical processes. *Angew Chem Int Ed Engl* **22**: 423–439.
35. Burgers, PM, Eckstein, F and Hunneman, DH (1979). Stereochemistry of hydrolysis by snake venom phosphodiesterase. *J Biol Chem* **254**: 7476–7478.
36. Spitzer, S and Eckstein, F (1988). Inhibition of deoxyribonucleases by phosphorothioate groups in oligodeoxyribonucleotides. *Nucleic Acids Res* **16**: 11691–11704.
37. Schroeder, SJ and Turner, DH (2009). Optical melting measurements of nucleic acid thermodynamics. *Meth Enzymol* **468**: 371–387.
38. Marky, LA and Breslauer, KJ (1987). Calculating thermodynamic data for transitions of any molecularity from equilibrium melting curves. *Biopolymers* **26**: 1601–1620.
39. Stellwagen, E, Renze, A and Stellwagen, NC (2007). Capillary electrophoresis is a sensitive monitor of the hairpin-random coil transition in DNA oligomers. *Anal Biochem* **365**: 103–110.
40. Straarup, EM, Fisker, N, Hedtjärn, M, Lindholm, MW, Rosenbohm, C, Aarup, V *et al.* (2010). Short locked nucleic acid antisense oligonucleotides potently reduce apolipoprotein B mRNA and serum cholesterol in mice and non-human primates. *Nucleic Acids Res* **38**: 7100–7111.
41. Judge, AD, Bola, G, Lee, AC and MacLachlan, I (2006). Design of noninflammatory synthetic siRNA mediating potent gene silencing in vivo. *Mol Ther* **13**: 494–505.
42. Levin, AA (1999). A review of the issues in the pharmacokinetics and toxicology of phosphorothioate antisense oligonucleotides. *Biochim Biophys Acta* **1489**: 69–84.
43. Hartmann, G and Krieg, AM (2000). Mechanism and function of a newly identified CpG DNA motif in human primary B cells. *J Immunol* **164**: 944–953.
44. Parker, JS, Roe, SM and Barford, D (2005). Structural insights into mRNA recognition from a PIWI domain-siRNA guide complex. *Nature* **434**: 663–666.
45. Obad, S, dos Santos, CO, Petri, A, Heidenblad, M, Broom, O, Ruse, C *et al.* (2011). Silencing of microRNA families by seed-targeting tiny LNAs. *Nat Genet* **43**: 371–378.
46. Fasman, GD. *Handbook of Biochemistry and Molecular Biology, Vol 1: 589.* CRC Press: Boca Raton, FL, 1975.
47. Owczarzy, R, You, Y, Moreira, BG, Manthey, JA, Huang, L, Behlke, MA *et al.* (2004). Effects of sodium ions on DNA duplex oligomers: improved predictions of melting temperatures. *Biochemistry* **43**: 3537–3554.
48. Moreira, BG, You, Y, Behlke, MA and Owczarzy, R (2005). Effects of fluorescent dyes, quenchers, and dangling ends on DNA duplex stability. *Biochem Biophys Res Commun* **327**: 473–484.
49. Pohl, FM (1974). Thermodynamics of the helix-coil transition of (dG-dC) oligomers. *Eur J Biochem* **42**: 495–504.
50. Hail, ME, Elliott, B and Anderson, K (2004). High-throughput analysis of oligonucleotides using automated electrospray ionization mass spectrometry. *Am Biotechnol Lab* **4**: 12–14.

Supplementary Information accompanies this paper on the Molecular Therapy–Nucleic Acids website (http://www.nature.com/mtna)